Defining and Evaluating Production Capacity for the Northern Guam Lens Aquifer

Daniel V.G. Superales

Nathan C. Habana

John W. Jenson

WATER AND ENVIRONMENTAL RESEARCH INSTITUTE
OF THE WESTERN PACIFIC
UNIVERSITY OF GUAM

Technical Report No. 170

December 2019

DEFINING AND EVALUATING PRODUCTION CAPACITY
FOR THE
NORTHERN GUAM LENS AQUIFER

by
Daniel V.G. Superales
Nathan C. Habana
John W. Jenson

Water and Environmental Research Institute of the Western Pacific
University of Guam UOG Station, Mangilao, Guam 96923

Technical Report No. 170
December 2019

Acknowledgements: This project was funded by the Guam Hydrologic Survey (Guam Public Law 24-247). Dr. Stephen B. Gingerich, USGS Pacific Islands Water Science Center (now at the USGS Oregon Water Science Center) advised and assisted on the configuration and application of the modeling software.

ABSTRACT

A numerical groundwater model of the Northern Guam Lens Aquifer (Gingerich 2013) was used to evaluate the potential capacity of the freshwater lens. The current actual production system has about 130 wells, of which 48 are set on the parabasal zone. In this study, 130 vertical wells with screened depths of 40 feet were simulated exclusively within the parabasal zone, the portion of the freshwater lens that is supported by the volcanic basement rather than seawater, in successive average-pumping scenarios from 100 gpm to 500 gpm. Baseline simulation results produced about 42 MGD (million gallons per day) freshwater with a weighted-average chloride concentration of 44 mg/L, a 64% improvement over the current actual production system. Successive simulation results show that up to 89 MGD can be extracted from the aquifer while maintaining the weighted-average chloride concentration at ≤ 250 mg/L, the secondary drinking water guideline set by the U.S. and Guam Environmental Protection Agencies. These results show the advantage of focusing development of carbonate island karst aquifers on the parabasal zone.

Table of Contents

List of Figures

Chapter 1
INTRODUCTION

Guam's freshwater demand from the Northern Guam Lens Aquifer (NGLA) is expected to increase soon to accommodate development and population growth driven by military realignment and the expanding tourism industry. This study provides insights for sustainable management of the island's water resource. More than 100 production wells penetrate deep through the limestone plateau of northern Guam to reach the freshwater lens and pump out some 40 MGD, more than 90% of the island's freshwater consumption. Placement of these wells is key to optimizing the extraction and distribution system production, sustainably manage freshwater production, and obtaining sustainable freshwater yields. McDonald and Jenson (2003) and Simard et al. (2015) documented the relationship of salinity patterns and trends to well depths, pumping rates and hydrogeology in the NGLA. Their studies confirmed that wells in the parabasal zone (Fig. 1.1) are less susceptible to saltwater contamination than wells in the basal zone and are positioned to capture water flowing seaward from the suprabasal zone. The objective of this modeling study was to compare the potential performance of a hypothetical production system focused on the parabasal zone with that of the current actual system.

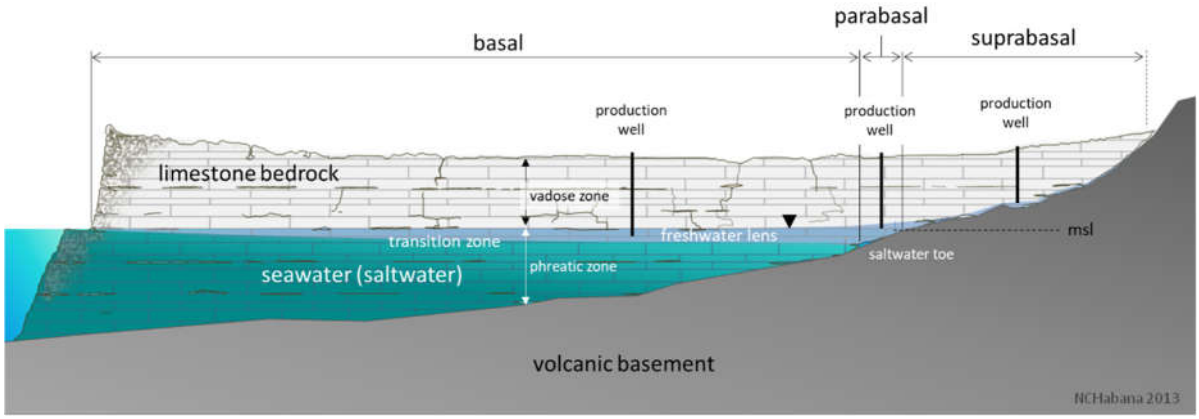

Fig. 1.1 Cross-section schematic diagram of the NGLA. Production wells are located over three groundwater zones (basal, parabasal, suprabasal). The vadose zone extends from the ground surface to the surface of the freshwater lens below and may be partially saturated from water percolating from the surface. The phreatic zone extends from the freshwater lens surface to the volcanic basement and is completely saturated with water. The basal zone is the portion of the freshwater lens that is below mean sea level (msl), underlain by the transition zone and seawater. The parabasal zone is the portion of the lens below msl and underlain by the volcanic basement between the saltwater toe (the intersection of the 50% isochlor and basement rock) and msl-basement boundary. The suprabasal zone contains freshwater flowing down to the basement slope above mean sea level.

1.1 The Northern Guam Lens Aquifer

Guam is the largest and southernmost island of the Mariana island chain. The island is located at 13°26'N. and 144°45'E, 1500 miles south of Tokyo, 1600 miles east of Manila

(Fig. 1.2). The total area is 211 mi^2 and is divided at the Pago-Adelup Fault as northern and southern physiographic regions: the northern plateau (102 mi^2); and southern volcanic upland (109 mi^2). Because the NGLA supplies 90% of Guam's potable water, it is designated by the USEPA as the island's sole source aquifer (USEPA 1978). The other 10% percent is from surface water and freshwater springs located in southern Guam.

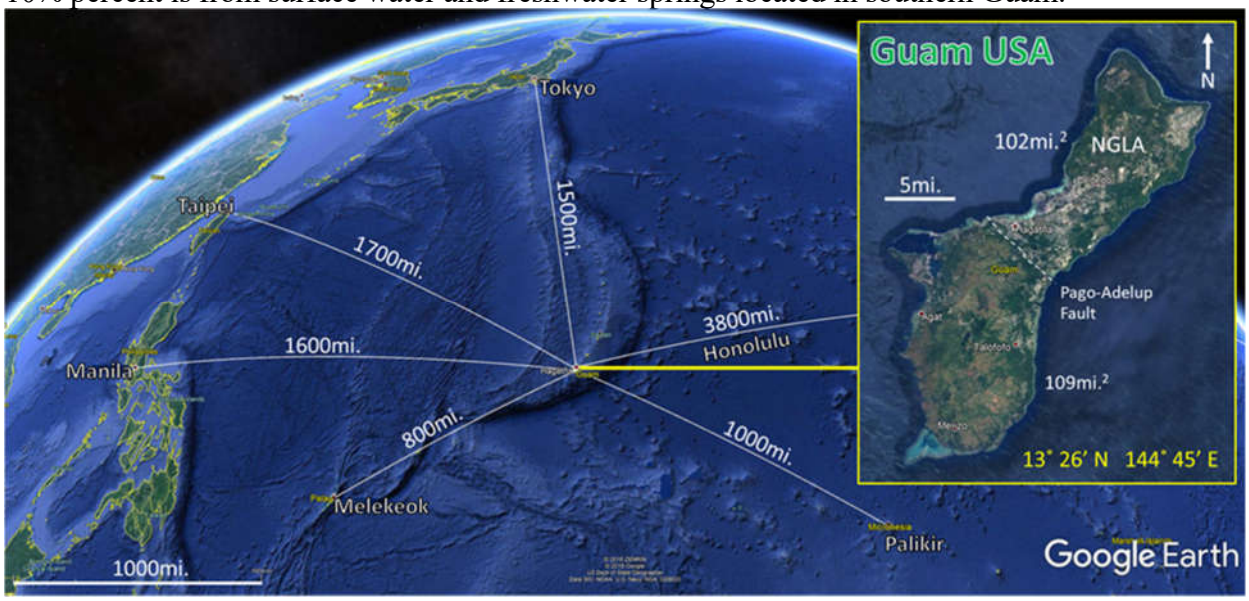

Fig. 1.2 Guam, southernmost island of the Mariana archipelago in the western North Pacific Ocean.

Nearly all the water produced from the NGLA is from vertical wells set from 25 to 50 ft screened depth, except for one horizontal (Maui style) 1000-ft tunnel well (Tumon-Maui Well), which produces about 1 MGD.

Groundwater development began in 1937 (CDM 1982), with the installation of seven production wells. After the successful extraction of aquifer water in the north in the 1960s and 1970s, groundwater was considered a promising means for development of the island's water supply (Barrett Consulting Group and Mink 1992). Current demand has since increased to 40-42 MGD, with Department of Defense, Guam Waterworks Authority (GWA), and private owners managing a total of about 130 production wells. Although it is an excellent renewable water source, groundwater production is ultimately limited by recharge and saltwater intrusion.

1.2 Water Resource Concern

The island's freshwater production currently supports a permanent resident population of about 170,000 including 12,000 military personnel and family members (Joint Military Installations 2020), and hosts 1.5 million tourists a year (Guam Visitor's Bureau 2018). Due to a planned military realignment, the island's population is expected to increase (Joint Guam Program Office 2010). Policy makers and water resource managers must know the quantity of freshwater that can be sustainably produced as demand for freshwater increases. John Mink (Barrett Consulting Group and Mink 1992) estimated that 80 MGD of acceptable quality water could be extracted sustainably if wells were placed in

optimal locations. This study builds on earlier hydrogeologic assessments (Contractor et al. 1981; Jocson et al. 1999; Mylroie et al. 1999; McDonald and Jenson 2003; Bendixson 2013; Vann et al. 2014; Simard et al. 2015) of the NGLA to evaluate the potential sustainable yield from optimal placement. The approach taken is to investigate how production could be optimized by redistributing the same number of wells, with the same construction entirely to the parabasal zone.

1.3 Need, Value, and Motivation for Model Investigation

Sustainable management of the aquifer requires basing decisions on reliable scientific investigations. In response to water availability concerns regarding the US Marines realignment, the US Navy approached the USGS Pacific Island Water Science Center (PIWSC), Hawaii, to develop a model of the NGLA to simulate hydrologic stress scenarios for additional wells (Gingerich and Jenson 2010). USGS PIWSC, in collaboration with WERI, had then constructed the most comprehensive and representative model of the NGLA to date (Gingerich 2013).

Determining the aquifer capacity and best practices for extracting fresh water requires geologic, hydrogeologic, and hydrologic perspective. From years of NGLA collaborative research, WERI is positioned to provide recommendations for optimum development and sustainable production. This study employed the 2013 model to determine the effects of concentrating production exclusively in the parabasal zone. This project is thus a first-phase exploration of the capacity of the aquifer's parabasal zone.

1.4 Purpose and Objectives

The goal of this project is to utilize a groundwater model to estimate the potential capacity of the parabasal zone for optimum development of the aquifer. This project utilizes the latest NGLA model (Gingerich, 2013) for configuring a production system comprised of parabasal wells and comparing results to the actual 2010 production system. The steps to achieve this goal are:

1. Determine a practical hypothetical well arrangement for the parabasal zone in the NGLA.
2. Run pumping simulations from 100 to 500 gpm, at 25 gpm increments, for wells with screened depths of 40 ft.
3. Apply model post-process analysis to compare the model results to the actual (2010) system performance.
4. Provide recommendations for aquifer management and development.

Recognizing that there could be many configurations to test aquifer capacity, the first three objectives were further delimited and defined based on related literature, regulations, as discussed in the next chapter. There the scope, limitations, and delimitations are identified and selected to describe the approach taken to suggest a best-practice configuration, while acknowledging that the best-practice configuration sets a benchmark that may never be achieved in actual practice.

Chapter 2
BACKGROUND AND RELATED RESEARCH

More than three decades of research and investment have brought together a groundwater model (Gingerich 2013) that can now be used to evaluate hypothetical sustainable management and optimum development scenarios for the NGLA. This chapter summarizes the up-to-date research on NGLA characteristics and properties, using the latest hydrogeologic map (Vann et al. 2015), decades of rainfall and hydrologic studies (Ward et al. 1965; Bendixson 2013), and records of production well performance (McDonald and Jenson 2003; Simard et al. 2015). Now, with the latest groundwater model available, the study here explores the production capacity of the NGLA.

2.1 The NGLA Characteristics and Properties

This section summarizes related research on the properties of the NGLA in terms of geology, hydrogeology, and hydrology.

2.1.1 Geology

The NGLA is a carbonate-island karst aquifer (Mylroie et al. 1999) beneath a limestone plateau. It is delineated north of the Pago-Adelup Fault (appendix 1), formed of two limestone units, mainly Barrigada (Miocene to Pliocene), which forms the core, and the younger Mariana Limestone (Pliocene to Pleistocene), which covers and surrounds the Barrigada Limestone core. The limestone is underlain by the Alutom Formation (Tracey Jr. et al. 1964), which forms the basement boundary of the aquifer and crops out at Mataguac Hill and Mount Santa Rosa. This limestone aquifer has been uplifted from its lagoonal and reef depositional environments, faulted and tilted, with surface elevations ranging from 200 to 500 ft.

2.1.2 Hydrogeology

The vadose zone extends from the plateau surface to the water table, and ranges from 200 to 600 ft thick. Groundwater recharge is infiltrated rainfall that descends through this thick vadose zone. The NGLA is composed of six hydrologically distinct basins (Fig. 2.5). Each basin constellates a separate watershed. The younger (Plio-Pleistocene) rock of Mariana Limestone covers and surrounds the older (Miocene-Pliocene) Barrigada Limestone of the aquifer core. The Mariana Limestone is a reef-lagoon deposit. The Barrigada Limestone is a granular, detrital foraminiferal deposit.

Within each basin are up to three groundwater zones: basal, parabasal, and suprabasal. The NGLA Map (appendix 2) shows a parabasal zone that occupies 5% of the aquifer, as determined from a no-pumping model (Gingerich, 2013) scenario. The base of the freshwater lens is defined where saltwater is calculated to be 50% seawater. Suprabasal occupies 25% of the aquifer.

2.1.3 Hydrology

The aquifer's freshwater lens is replenished with infiltrating rainfall that may percolate slowly or descend rapidly as vadose fast-flow (Mylroie et al. 1999). Recharge is the portion of rainfall that escapes evapotranspiration (ET). Johnson (2012) accounted for canopy evaporation, the ET rate for various land-cover types, and evaporation from impervious surfaces. Light to moderate rainfall infiltrates readily through the thin soil layer. Separate studies (Jocson et al. 1999; Partin et al. 2012; Beal et al. 2019) suggest that all the dry-season rainfall is consumed by (ET). Recharge only occurs during the wet season. Storm waters or intense rain may produce runoff and ponding when infiltration is exceeded, in which flow to surface depressions and sinkholes may channel large volumes of water through conduits and fractures that descend directly to the lens. The freshwater lens eventually carries water through the aquifer and discharges it at the coast.

Allogenic runoff from Mataguac Hill and Mt. Santa Rosa enters sinkholes found at the contact between the limestone aquifer and basement aquiclude, where it travels as suprabasal water until entering the parabasal zone. At the same time, autogenic recharge occurs as water percolates downward from the surface of the suprabasal and parabasal zones (Fig. 2.1 and appendix 2).

Recharge for the NGLA has been estimated from hydrologic models of water budget and spatial analysis (Jocson et al. 1999; Habana et al. 2009), and rainfall and groundwater chloride analysis (Ayers 1981). Ayers provided historic background to earlier methods for estimating recharge, which includes streamflow estimates from southern Guam, since the area there is nearly the same as in NGLA.

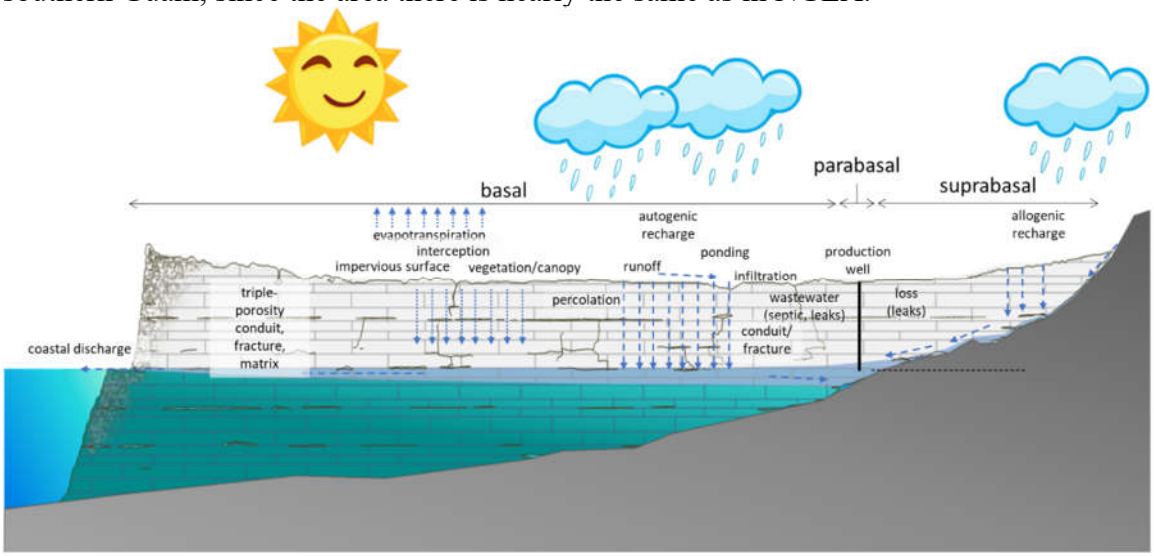

Fig. 2.1. Hydrologic cycle of the NGLA.

Mink estimated about 60% of rainfall goes to recharge (Camp Dresser and McKee Inc. 1982). Jocson et al. (1999) estimated 67% of rainfall goes to recharge. Based on a previous estimate from Johnson, (2012), 225 MGD was assigned as recharge to the NGLA model (Gingerich 2013).

A production well in the parabasal zone (Fig. 2.1) is less susceptible to saltwater intrusion as it is underlain by basement rock (Alutom Formation). The low permeability of the basement rock prevents the seawater from entering the freshwater lens above. However, pumping may thin the lens and move the saltwater toe towards mean sea level at the basement, changing the parabasal well into a basal well and increasing

susceptibility to saltwater intrusion. Water in the suprabasal zone eventually enters the parabasal zone. Thus, parabasal wells capture both parabasal and suprabasal water.

2.2 NGLA Production Well System and Management

Nearly all the utility water from the NGLA is pumped from vertical production wells that penetrate the thick vadose zone and generally 40 ft into the phreatic freshwater. More than 100 vertical production wells are installed (including 1 horizontal 1000-ft tunnel Tumon-Maui well) owned by DOD and operated by GWA. This section provides background on Guam's production wells, design and construction regulations, and performance that was used in determining the optimum well placement and parameter selection for the groundwater model analysis.

2.2.1 Production Wells

Production wells are constructed drilling deep vertical boreholes that penetrate the lens from 25 to 40 or 50 ft deep. It is then cased to prevent collapse. Louvered screens begin a few feet beneath the water table down to the bottom, to let water in, prevent large rocks from entering, and maximize exposure to water-bearing zones. The pump is at the bottom of the well, forcing all captured water to the surface.

2.2.2 Well Design, Construction, and Aquifer Capacity

Soon after the NGLA was determined in 1978 to be a sole source aquifer (US Environmental Protection Agency 1978), it was decided that the aquifer production limits and optimum development be explored. The 1982 Northern Guam Lens Study (CDM 1982) recommended regulations and guidelines to the Guam Environmental Protection Agency (US Environmental Protection Agency 2015) for production well development over the NGLA. Accordingly, GEPA regulates well design, setting maximum well depth to -40 feet below the "static" water level for basal wells and -50 ft for parabasal wells. Wells are screened from a few feet below the water table to the bottom of the borehole, generally 40 to 50 ft below the water table.

2.2.3 Previous Salinity Studies and Regulations

Water quality benchmarks for salinity were first proposed by John Mink for the 1982 Northern Guam Lens Study (Camp Dresser and McKee Inc. 1982) and were used by McDonald and Jenson (2003) — which is still the point of departure for groundwater evaluations on Guam. The regulatory limit on Guam, at least for now, is the GEPA secondary standard of 250 mg/L chloride (US Environmental Protection Agency 2015). World Health Organization guidelines suggest that up to 600 mg/L chloride can still be regarded as potable. However, Mink advised that the engineering target for water quality at each well be 150 mg/L chloride (Camp Dresser and McKee Inc. 1982)

Chloride vulnerability in basal zone was illustrated in Simard et al. (2015) (Fig. 2.2). Production wells thin the lens in (a), bringing up saline groundwater and pulling down on the water table. In (b), a well that causes drawdown and the classic up-coning, bringing up the saltwater beneath. In the NGLA, (c) and (d) is common, where fractures, fissures, and conduits dominate the draw direction. Well (c) is

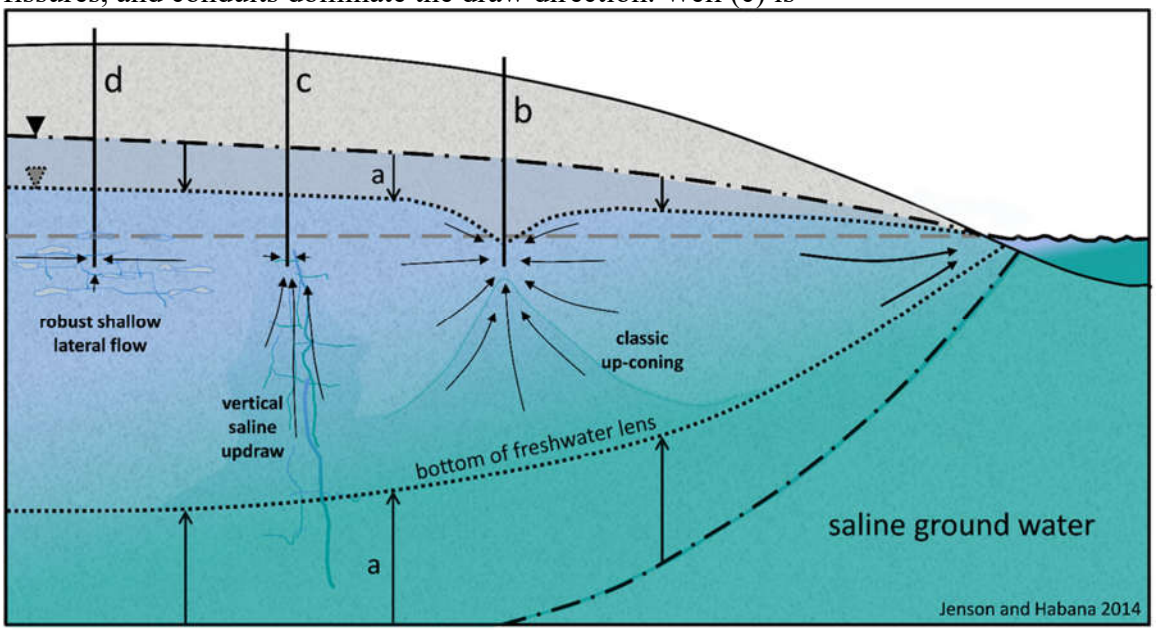

Fig. 2.2 Basal zone well production in NGLA (Simard et al. 2015)**.**

the least favorable as vertical saline updrawn that may have a direct pore, like a straw, into the saline groundwater. Well (d) however is desirable in basal wells, getting a robust and shallow lateral flow. In each case, there could be a drawdown if pump rate overwhelms the hydraulic conductivity. In the model however, we are limited by Darcian parameters, regional hydraulic conductivity, in which the only modeled well response can be the classic up-coning.

Production and chloride data analysis from McDonald and Jenson (2003) and Simard et al. (2015) have confirmed that wells located in the parabasal zone have the least susceptibility to salinity issues (Fig. 2.3). Wells are classified as basal, parabasal, or suprabasal according to the aquifer map of Vann et al (2014), in which the boundary of zones was based on Gingerich's model results (2013).

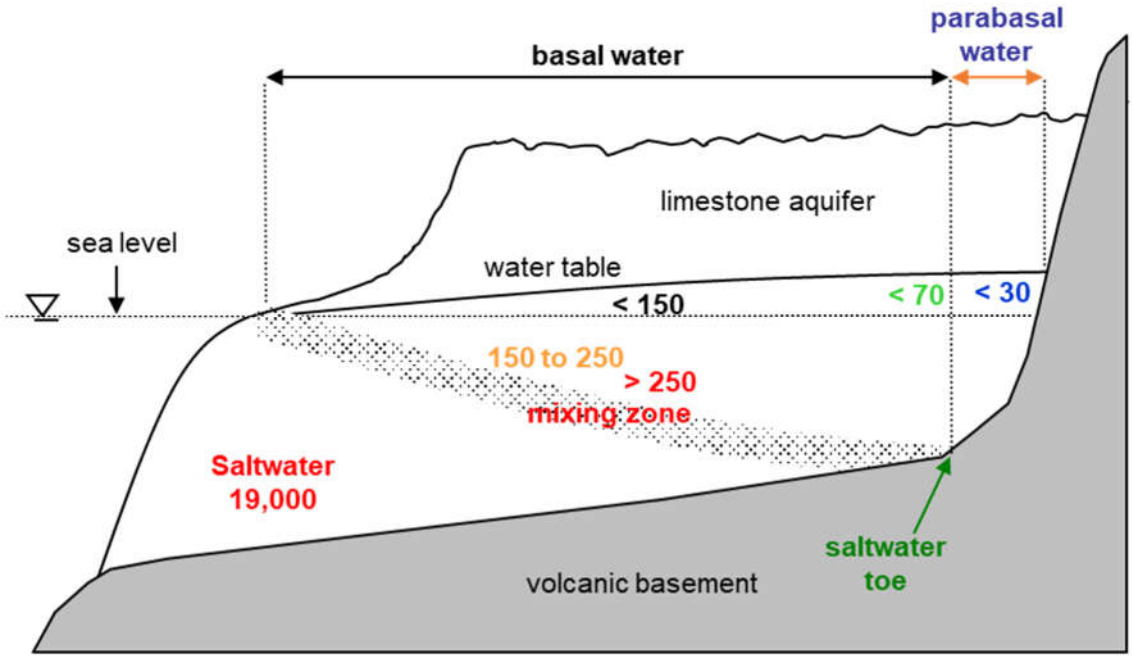

Fig. 2.3 Production well chloride range in areal groundwater zones (McDonald and Jenson 2003).

Top of the list for high production and low salinity wells are the suprabasal, spring, and horizontal (Maui style) wells. In overall descending order of favorable wells are parabasal, basal with lateral flow, basal up-coning, and the unlucky vertical saline updraw. Wells of low production and high salinity in the parabasal set may be basal wells, since the saltwater toe boundary of Vann et al. (2014) was based on a no pumping model scenario (Gingerich, 2013). Although suprabasal wells are freshest ($[Cl^-] < 30$ mg/L), it is very difficult to find productive locations in the suprabasal zone. The aquifer model is limited to the phreatic zone, below msl, so it does not include suprabasal wells.
Basal water is easy to find but is vulnerable to saltwater intrusion. So, it was determined that this project would test the capacity of the parabasal zone as a hypothetical exclusive zone of development.

Fig. 2.4 on the next page is a map of the NGLA basins and groundwater zones. The areal groundwater zones are teal for basal, blue for parabasal, and gray for suprabasal. The suprabasal zone contributes allogenic and autogenic recharge to the parabasal, accounting for about 53 sq. km (25% of 264 sq. km) and 51 in. per year of rainfall to recharge, which is about 62 MGD available. The 65 in. per year recharge would result in 79 MGD (recall Mink, 80 MGD).

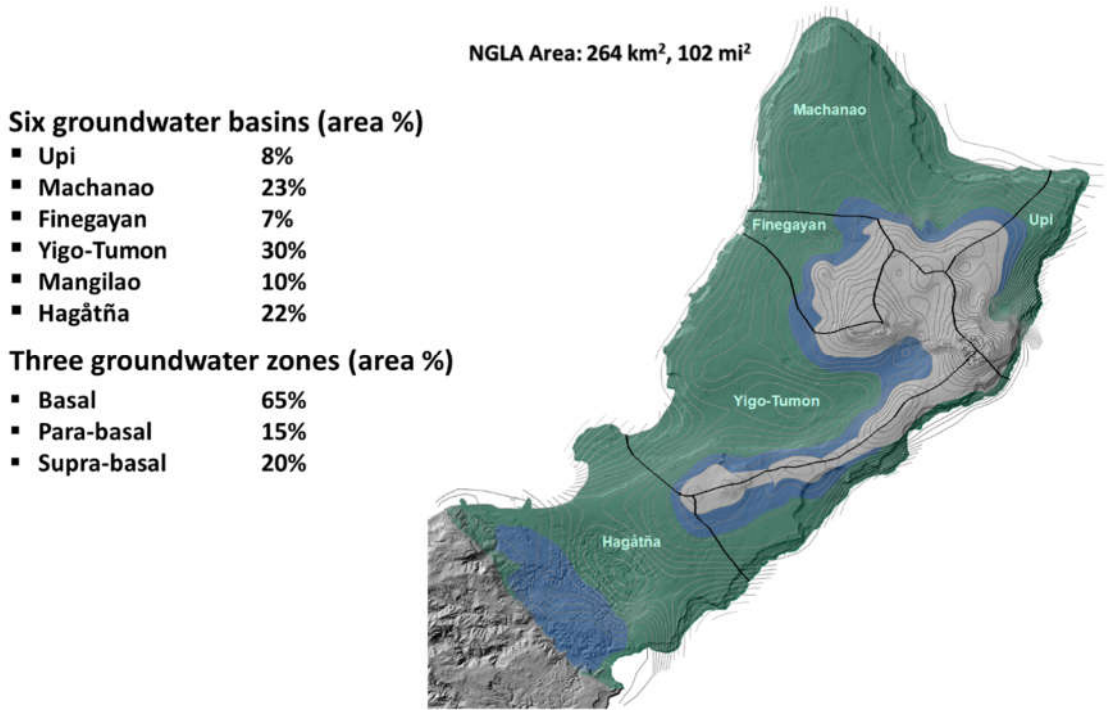

Fig. 2.4. Aquifer basins and groundwater zones.

Simard et al. (2015) compiled and analyzed the production well data from 2000-2010. The same dataset was used to define the average observed production system used to calibrate the NGLA model (Gingerich 2013). From that dataset, select wells were used to calculate the average pump rate (222 gpm).

2.3 NGLA Model

The latest and most comprehensive NGLA groundwater model was developed by USGS. Gingerich, 2013, in collaboration with WERI, developed a USGS SUTRA (version 2.2) (Voss and Provost, 2002, version of September 22, 2010), hybrid finite element model of the NGLA. The model is built from most recent data and much supportive analysis and collaboration. The collaborative research involved funding from USGS and P.L. 24-247 and 24-161 (GHS and CWMP, respectively).

- Johnson, 2012, Recharge, USGS
- Rotzoll et al 2019, Regional Hydraulic Conductivity, USGS
- Vann et al. 2014, Basement topography, USGS, GHS
- Bendixson et al. 2013, Borehole database, GHS, USGS
- Simard et al. 2015, Chloride analysis, GHS, USGS
- Observation well data, CWMP, USGS
- Jocson et al. 1999, Coastal discharge, GHS

All available and useful data have been thoroughly examined and applied to build the model.

2.4 Sustainable Yields, Development, and Management

Determining sustainable water production and appropriate management recommendations requires an economic analysis of production in addition to the hydrologic analysis of sources reported here. This stage of analysis is not the definitive answer to aquifer capacity, but it is a fundamental step that must precede an economic evaluation.

The parabasal zone is considered the aquifer's "sweet spot" as it is invulnerable to saltwater intrusion except when excessive pumping causes the saltwater toe to migrate upslope. It receives the most allogenic and autogenic recharge from the suprabasal zone, as well as direct autogenic infiltration and basement discharge. Wells in the parabasal zone can also draw adjacent basal groundwater. Optimum development is extracting from this maximum renewable sweet zone.

2.5 Scope, Limitations, Delimitations, and Assumptions

The NGLA may have multiple optimum well arrangements. The model is therefore delimited to keep it consistent with a realistic infrastructure and operating costs.

Scope: The domain of this study is the Northern Guam Lens Aquifer, which includes all six aquifer basins. This model was calibrated to production wells and observation wells. The NGLA model used is a phreatic, steady-state model that covers the basal and parabasal zones, but not the suprabasal. The zone of interest is the parabasal zone, which is compared with the observed (2015) system.

Limitations: It is recognized that the model operates on Darcian and regional-scale parameters. Karst aquifers have discrete, localized, and spatially varied porosity and flow paths that cannot be incorporated, however, the NGLA model used is still acceptable for estimating the aquifer's capacity at the regional scale. All limitations of the model are recognized in supporting research, and approximated and averaged especially where data are limited.

Delimitations: Delimitations were necessary, otherwise, there could have been an infinite combination of well configurations and settings. The major variables of interest are the setting of well pump rates (gpm) and chloride concentration (mg/L) as seawater salinity. A major delimitation was the use of practical and common vertical production wells. The well settings for the model are based on maximizing the regulatory well depth, below msl, (40', 12.2 m) and use of full screening. The model uses 130 wells, which is about the maximum number of wells used in the observed production system (2010) in the Simard et al. (2015) study. Simulated well pump rates were uniform, starting with the average, to start from the observed 2015 total yield, 42 MGD. The first step was to determine a parabasal model well placement configuration with the average pump rate. The use of steady-state simulation is adequate as it approximates long term freshwater withdrawal. Furthermore, while other contaminants may limit or even halt water production (below minimum demand rate), this project focuses on pump rate limited by saltwater intrusion (chloride concentrations) only, as it is the most expected chemical species to increase with pump rate from saline up-coning.

Assumptions: This project assumes that land use and property constraints in the parabasal zone are no issue.

2.6 Objective Refinement

The objectives in Chapter 1 are thus refined as follows:

1. Initial conditions (baseline) determine a practical parabasal well placement configuration with the following conditions based on the practical settings:
    - Arrange 130 wells in the parabasal zone in all 6 basins.
    - Set the well depths to -40ft below msl.
    - Set each well to pump at the average pump rate of wells in the actual 2010 system.
    - Run to steady state, post process, and examine resulting chloride concentrations.
    - If chloride concentration at the well is greater than 250 mg/L, relocate the well within the parabasal zone and repeat the previous step.

2. Using the baseline configuration, run 17 additional simulations, setting all wells to the same pump rates from 100 to 500 gpm in increments of 25 gpm.

3. Analyze and interpret results
    - Graph production rate compared with chloride concentration for each basin and for the entire aquifer.
    - Produce chloride maps for each pumping scenario.
    - Summarize the results as composite concentration, or volume-weighted average chloride concentration (Gingerich 2019), for each basin and the NGLA for each pumping scenario.
    - Interpret results and distinguish from the observed system.

Chapter 3
METHODS

This chapter discusses the data used, model scenarios, and statistical and graphical analyses.

3.1 Data

The dependent variable for simulations is chloride concentration (mg/L). Equivalent chloride concentrations were converted from simulated salinity values, expressed as a weighted percentage of seawater, in the SUTRA output by dividing by the global mean salt-to-sea water ratio (0.0357) (Pilson 2013) and multiplying the result by the global mean chloride concentration (19,600 mg/L). Individual production wells were grouped into five categories based on prior studies (McDonald and Jenson 2003; Gingerich 2013) and using descriptors from Simard et al. (2015) and Gingerich (2013): threatened (> 500 mg/L chloride), out of standard (>=250 and <500 mg/L chloride), marginal (>=150 and <250 chloride), standard (>= 70 and <150 mg/L chloride), or good (>= 30 and <70 mg/L chloride). Gingerich (2013) assigned model recharge a chloride concentration of 30 mg/L. Anomalous simulated chloride concentrations for simulated wells less than recharge are due to numerical instability and are reset to the baseline value of 30 mg/L.

The model uses a uniform pump rate across all simulated wells. The independent variable is pump rate.

Shape files containing the NGLA model mesh (Gingerich 2013), Northern Guam boundaries, parabasal boundaries (i.e., saltwater toe and sea level contour), volcanic basement contours, and regional hydraulic conductivity were imported into Geographic Information System (GIS), ESRI® ArcMap 10.6, where well locations and attribute/parameter settings were assigned.

Well production and salinity data from the data set used to calibrate the NGLA model (Gingerich 2013) were used to define the actual system used in this study. AF-series, suprabasal, and non-drinking water wells were excluded. A summary table and chloride map for this data set is shown in Chapter 4 (Table 4.1).

3.2 Average Pump Rate Scenario

Production well locations were assigned by GIS. The calibrated NGLA model (Gingerich 2013) mesh was exported from ARGUSONE and the SUTRA graphical user interface and imported to GIS. 130 groundwater model wells were placed or about the parabasal zones over all 6 aquifer basins (Fig. 3.1). A well-naming convention was used to identify for each well its basin, groundwater zone, tier, and series (Fig. 3.1). The well location shape file was then imported to SUTRA for further configuration. The depth of each simulated well was set at 40 ft below msl elevation and assumed fully screened. Each simulated well was configured to withdraw at the 2010 system average pump rate of 222 gpm. In the Hagåtña basin, initial simulations resulted in wells with chloride concentrations greater than 250 mg/L. Those wells were removed and assigned to other basins until the simulation resulted in all wells with concentrations below 250mg/L.

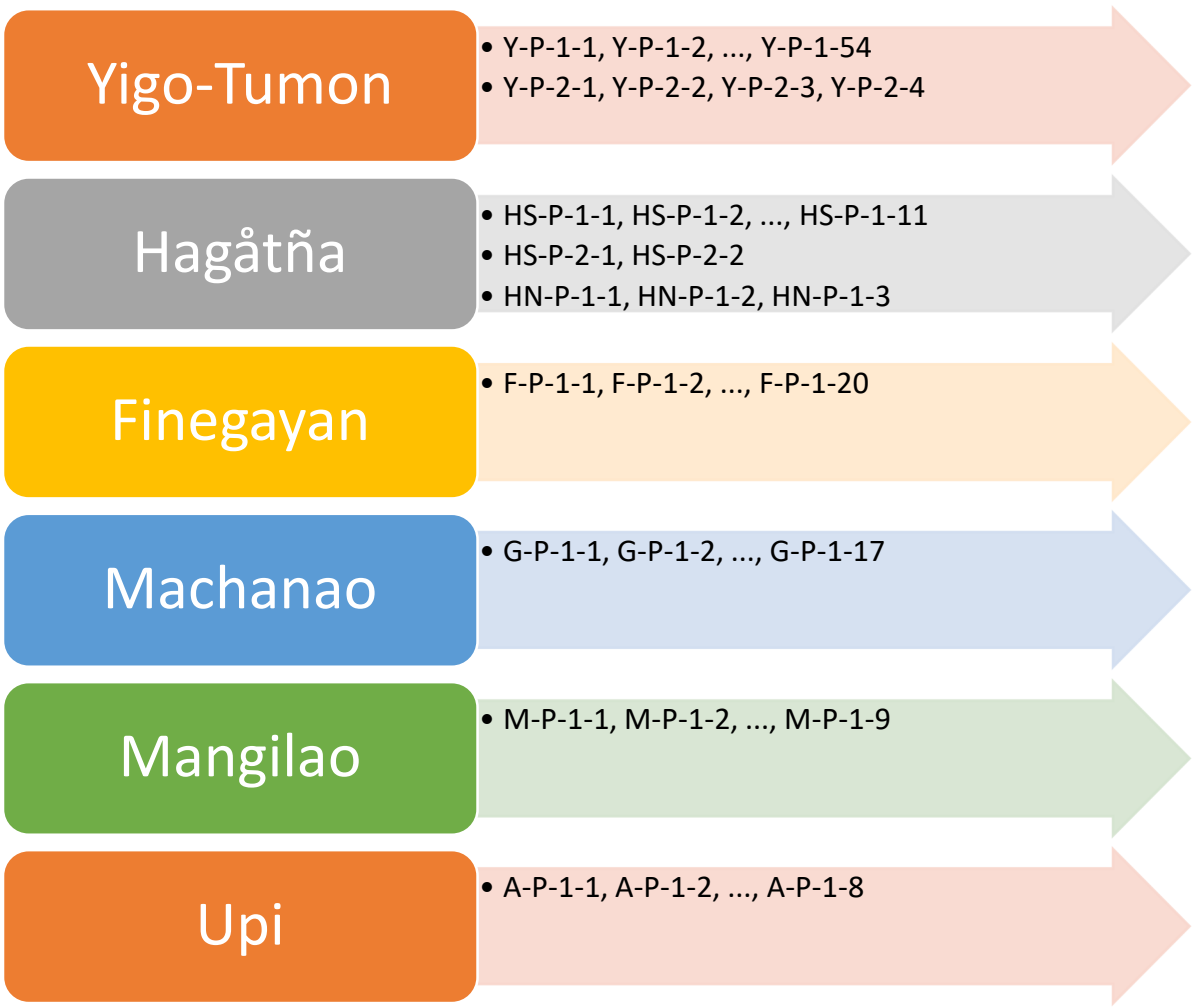

Fig. 3.1 Naming convention used for each modeled well. The hyphen-delimited naming convention identifies basin, groundwater zone, tier, and serial number.

3.3 100 gpm-500 gpm scenarios

Using the baseline configuration (Fig. 3.1), seventeen simulations were executed, starting at configuring all simulated wells to pump at 100 gpm, incrementing by 25 gpm, up to 500 gpm.

3.4 Statistical and graphic analyses

The results for each pumping scenario were then imported in GIS and simulated weighted-average chloride concentration for each well was color coded as previously mentioned in section 3.1. Anomalous simulated negative chloride concentrations, subsequently set to 30 mg/L, are represented by hollow light blue circles. Simulated chloride concentrations greater than 500 mg/L are represented by purple dots.

The resulting data for all 18 pumping scenarios were arranged for graphic analysis using Microsoft® Excel, comparing pump rate with chloride concentration in a line chart for each basin and the entire NGLA. Using spreadsheets, the composite concentration was calculated for each basin and the NGLA. Finally, summary tables for the actual system and the scenario results were created.

Chapter 4
RESULTS

Production vs. chloride concentration charts, GIS chloride maps, and summary tables were created to show the results of the parabasal zone pumping simulations from 100-500 gpm.

4.1 Actual System Conditions

A chloride map of the current actual system containing 121 total production wells, which Gingerich (2013) used as baseline is shown in Fig. 4.1. 48 production wells (40%) are located within the parabasal zone. 73 production wells (60%) are located within the basal zone. Comparisons between the actual and simulated production systems are discussed in the next chapter.

4.2 Baseline Scenario

Fig. 4.2 is a chloride map of the NGLA representing the results of the baseline simulation at 222 gpm. A summary table detailing the chloride concentration benchmark count is shown directly below the map. Thirty percent of simulated wells (39) have weighted average chloride concentrations below 30 mg/L; hence are set to 30 mg/L. Simulated parabasal wells with chloride concentrations greater than 500 mg/L use the "Threatened" descriptor adopted from Gingerich (2013). Below the benchmark table is a summary table detailing for each basin the number of wells, total pump rate (gpm and MGD), average pump rate and average weighted chloride concentration.

4.3 100-500 gpm Pump Rate Scenarios

Additional chloride maps and summary tables (Fig. 4.3-4.19) were produced similarly to the baseline scenario map. These maps illustrate the change, if any, in the weighted average chloride concentration benchmark per simulated production well for each pumping scenario. The baseline scenario chloride map (Fig. 4.1) is identical to the 225 gpm scenario map (Fig. 4.8).

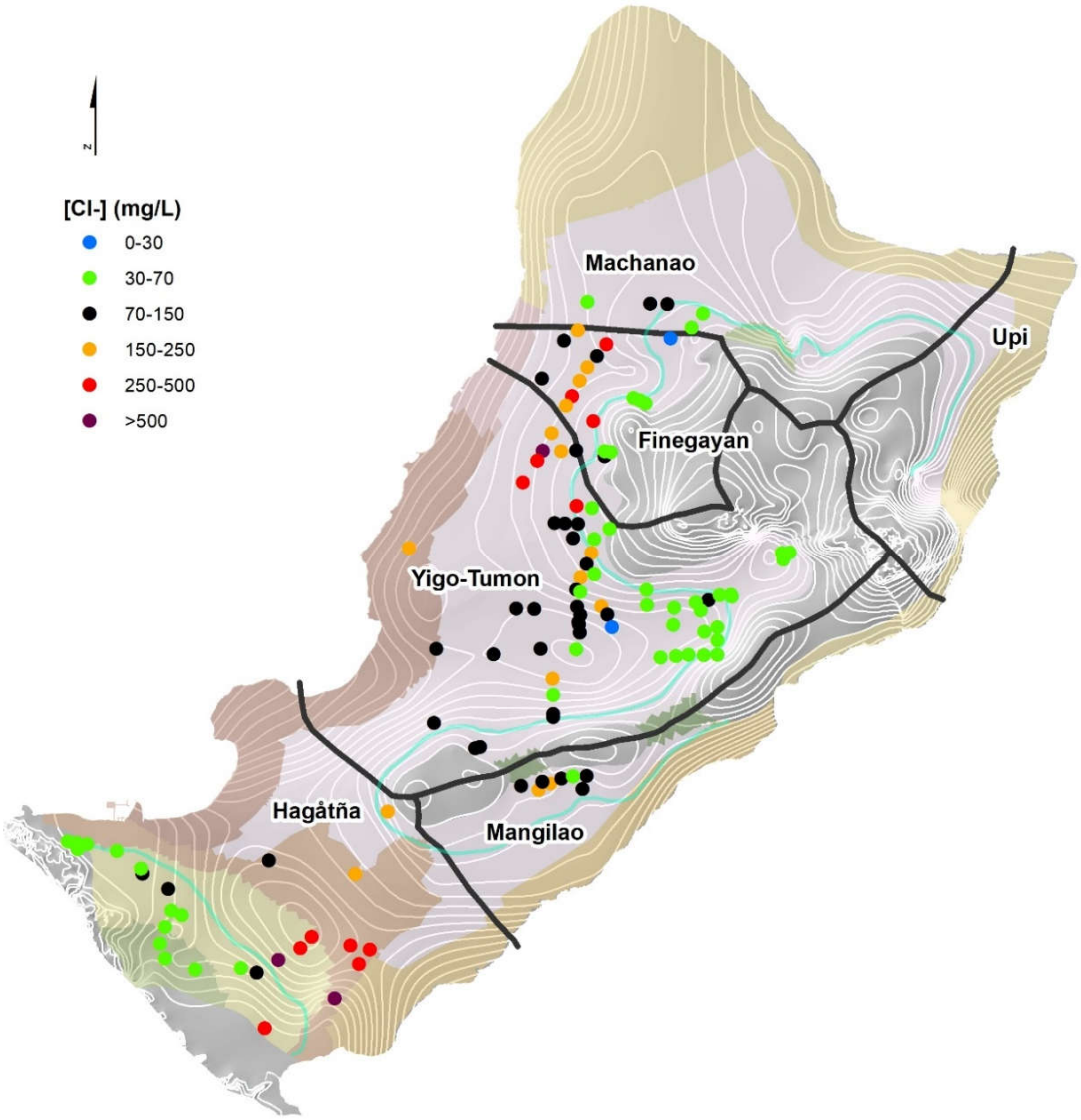

Fig. 4.1 Actual system NGLA chloride map.

Benchmark Count	<30 mg/L	Good	Standard	Marginal	Out of Standard	Threatened
	2	49	40	15	12	3

Basin	No. of Wells	Total Pump Rate (GPM)	Total Pump Rate (MGD)	Average Pump Rate (GPM)	Average [Cl-] (mg/L)
Machanao	5	967	1	193	58
Upi	0	0	0	0	0
Finegayan	18	3526	5	196	123
Yigo-Tumon	63	14589	21	232	98
Mangilao	8	1506	2	188	105
Hagåtña	27	6224	9	231	197
NGLA	121	26812	39	222	123

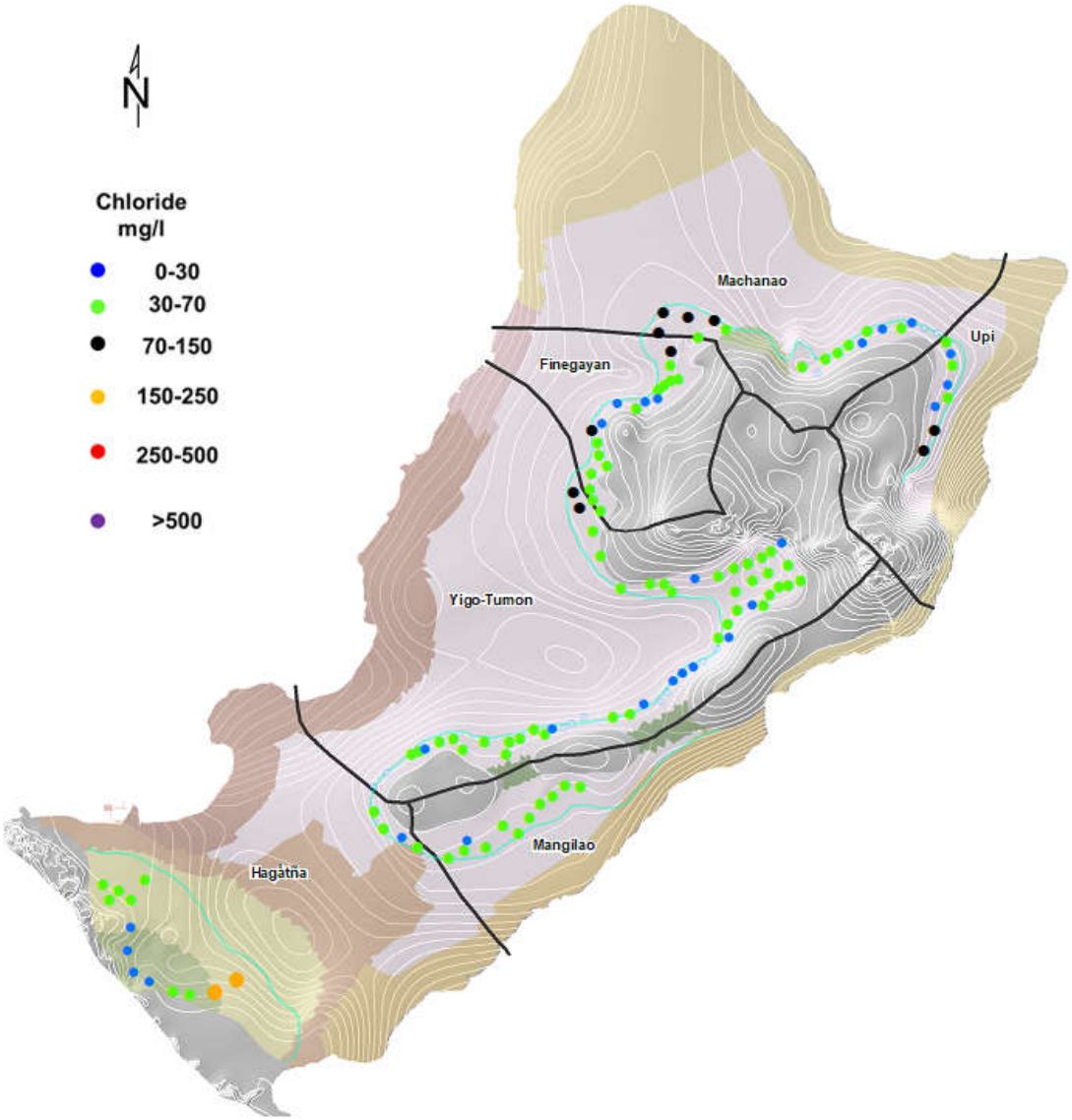

Fig. 4.2 Baseline scenario NGLA chloride map.

Benchmark Count	<30 mg/L	Good	Standard	Marginal	Out of Standard	Threatened
	39	79	10	2	0	0

Basin	No. of Wells	Total Pump Rate (GPM)	Total Pump Rate (MGD)	Average Pump Rate (GPM)	Average [Cl-] (mg/L)
Machanao	17	3774	5	222	53
Upi	8	1776	3	222	52
Finegayan	20	4440	6	222	40
Yigo-Tumon	57	12654	18	222	39
Mangilao	11	2442	4	222	35
Hagåtña	17	3774	5	222	57
NGLA	130	28860	42	222	44

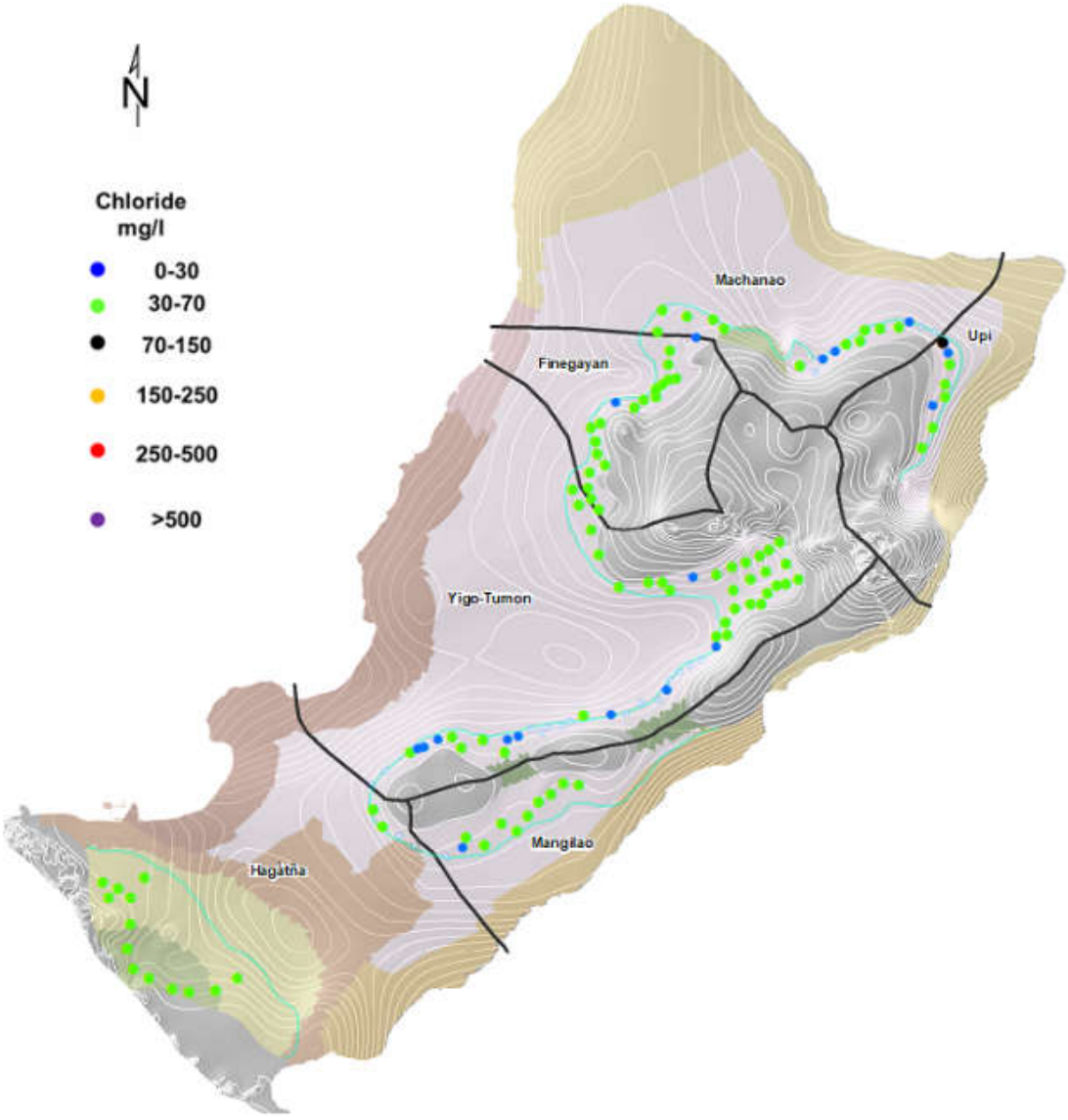

Fig. 4.3 100 gpm scenario NGLA chloride map with summary table.

Benchmark Count	<30 mg/L	Good	Standard	Marginal	Out of Standard	Threatened
	37	92	1	0	0	0

Basin	No. of Wells	Total Pump Rate (GPM)	Total Pump Rate (MGD)	Average Pump Rate (GPM)	Average [Cl-] (mg/L)
Machanao	17	1700	2	100	39
Upi	8	800	1	100	46
Finegayan	20	2000	3	100	33
Yigo-Tumon	57	5700	8	100	33
Mangilao	11	1100	2	100	33
Hagåtña	17	1700	2	100	37
NGLA	130	13000	19	100	35

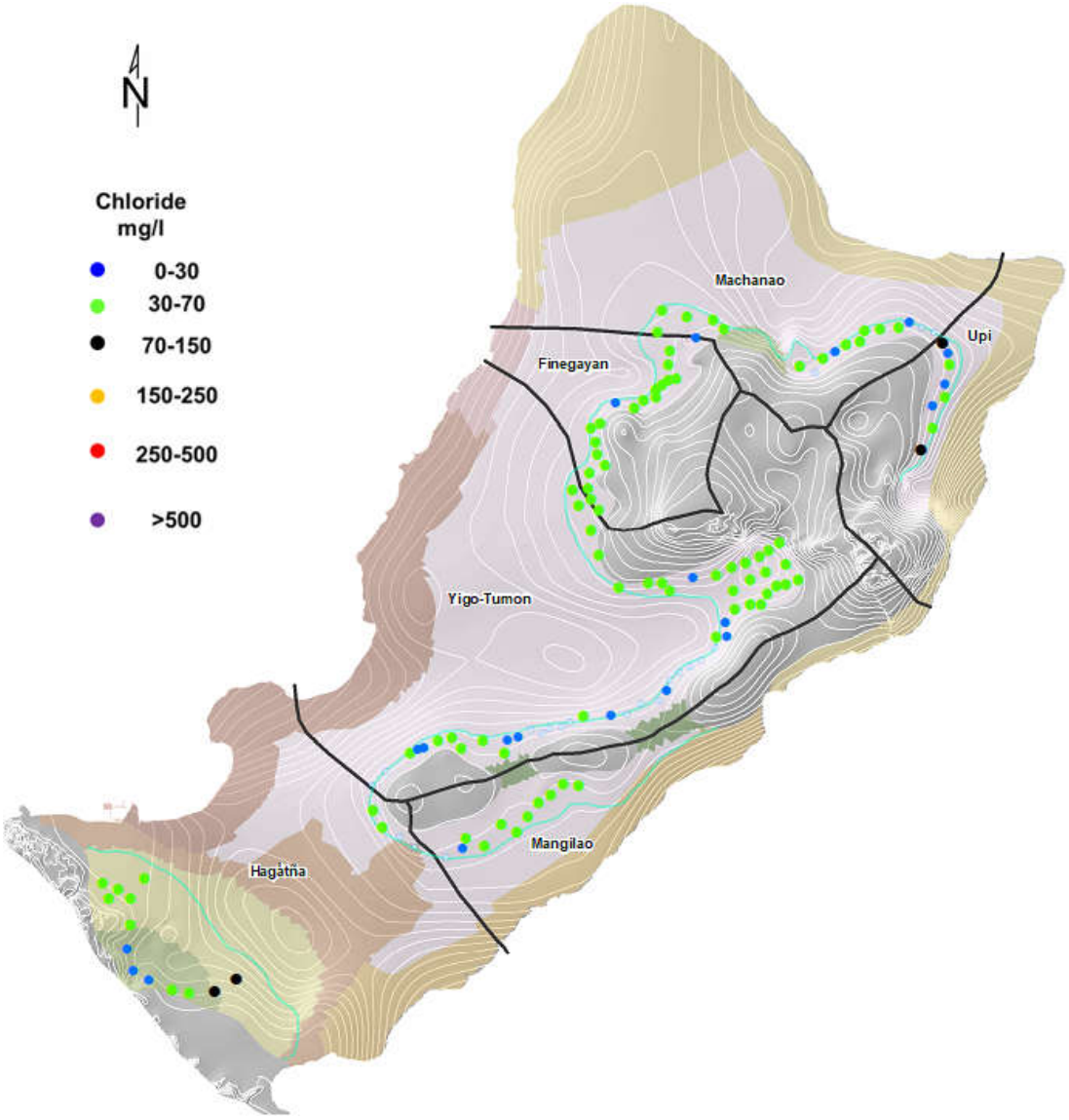

Fig. 4.4 125 gpm scenario NGLA chloride map.

Benchmark Count	<30 mg/L	Good	Standard	Marginal	Out of Standard	Threatened
	41	85	4	0	0	0

Basin	No. of Wells	Total Pump Rate (GPM)	Total Pump Rate (MGD)	Average Pump Rate (GPM)	Average [Cl-] (mg/L)
Machanao	17	2125	3	125	41
Upi	8	1000	1	125	47
Finegayan	20	2500	4	125	33
Yigo-Tumon	57	7125	10	125	33
Mangilao	11	1375	2	125	33
Hagåtña	17	2125	3	125	39
NGLA	130	16250	23	125	36

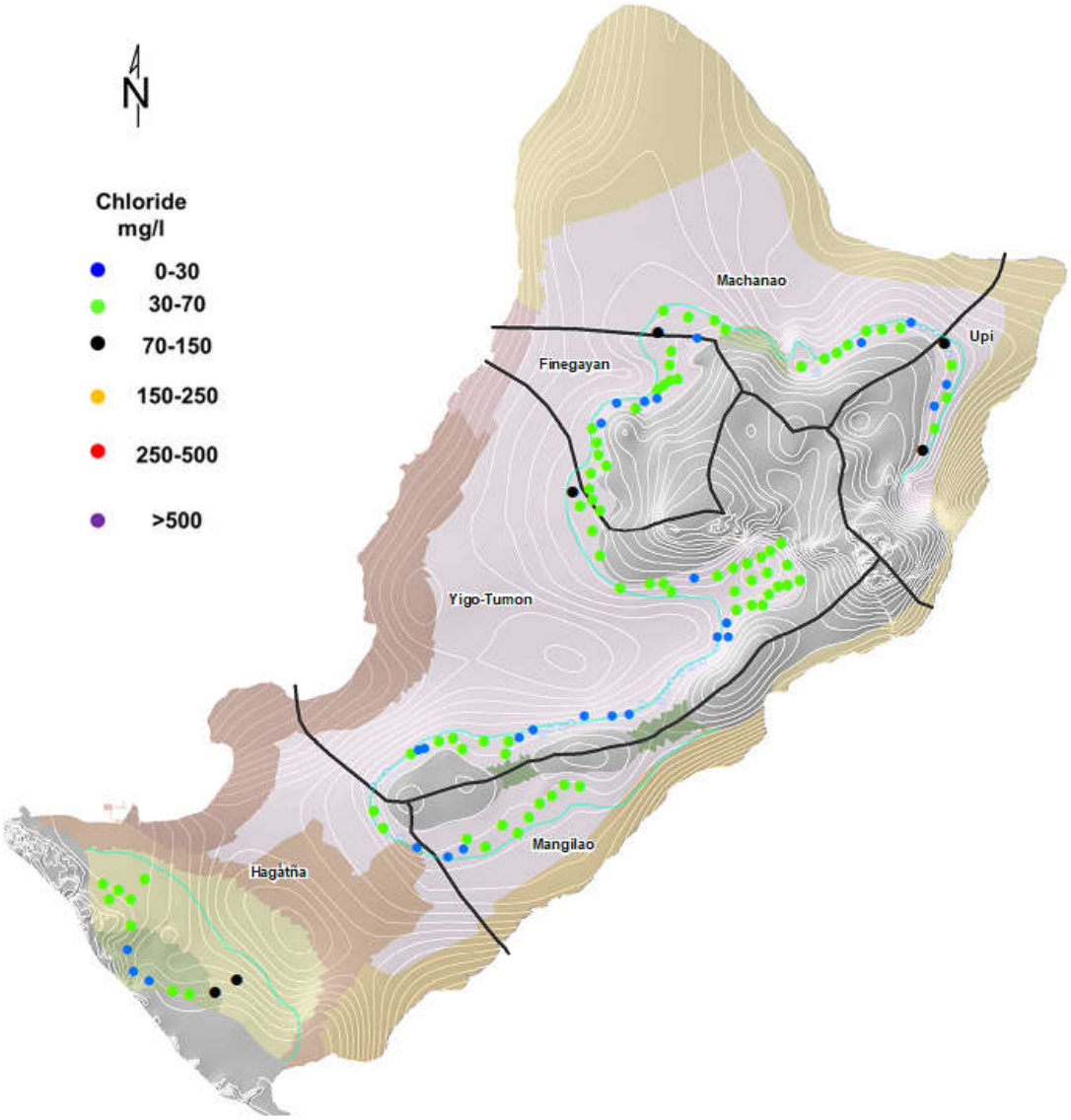

Fig. 4.5 150 gpm scenario NGLA chloride map.

Benchmark Count	<30 mg/L	Good	Standard	Marginal	Out of Standard	Threatened
	45	79	6	0	0	0

Basin	No. of Wells	Total Pump Rate (GPM)	Total Pump Rate (MGD)	Average Pump Rate (GPM)	Average [Cl-] (mg/L)
Machanao	17	2550	4	150	43
Upi	8	1200	2	150	48
Finegayan	20	3000	4	150	33
Yigo-Tumon	57	8550	12	150	34
Mangilao	11	1650	2	150	33
Hagåtña	17	2550	4	150	42
NGLA	130	19500	28	150	37

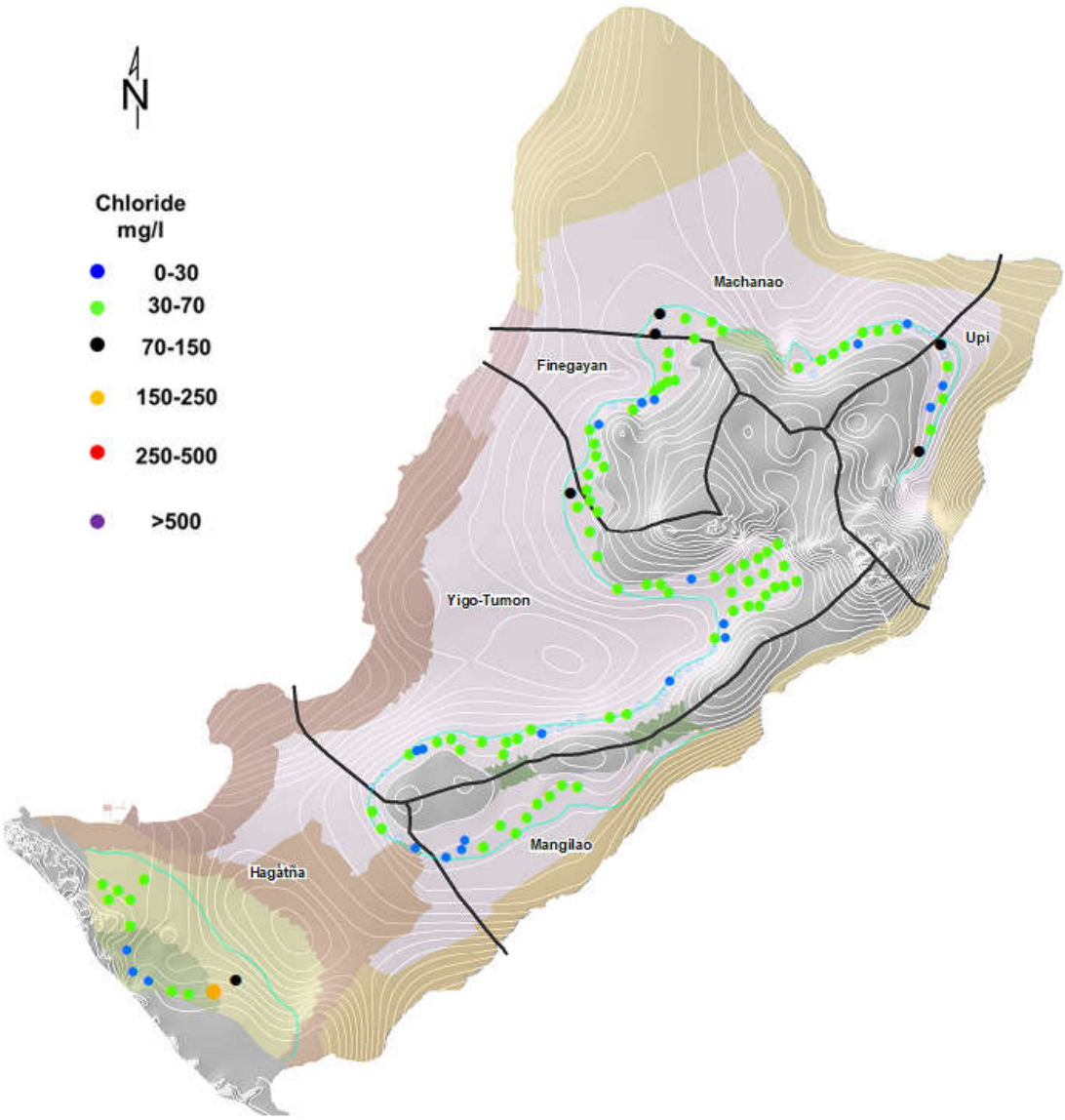

Fig. 4.6 175 gpm scenario NGLA chloride map.

Benchmark Count	<30 mg/L	Good	Standard	Marginal	Out of Standard	Threatened
	40	83	6	1	0	0

Basin	No. of Wells	Total Pump Rate (GPM)	Total Pump Rate (MGD)	Average Pump Rate (GPM)	Average [Cl-] (mg/L)
Machanao	17	2975	4	175	46
Upi	8	1400	2	175	49
Finegayan	20	3500	5	175	36
Yigo-Tumon	57	9975	14	175	35
Mangilao	11	1925	3	175	33
Hagåtña	17	2975	4	175	46
NGLA	130	22750	33	175	39

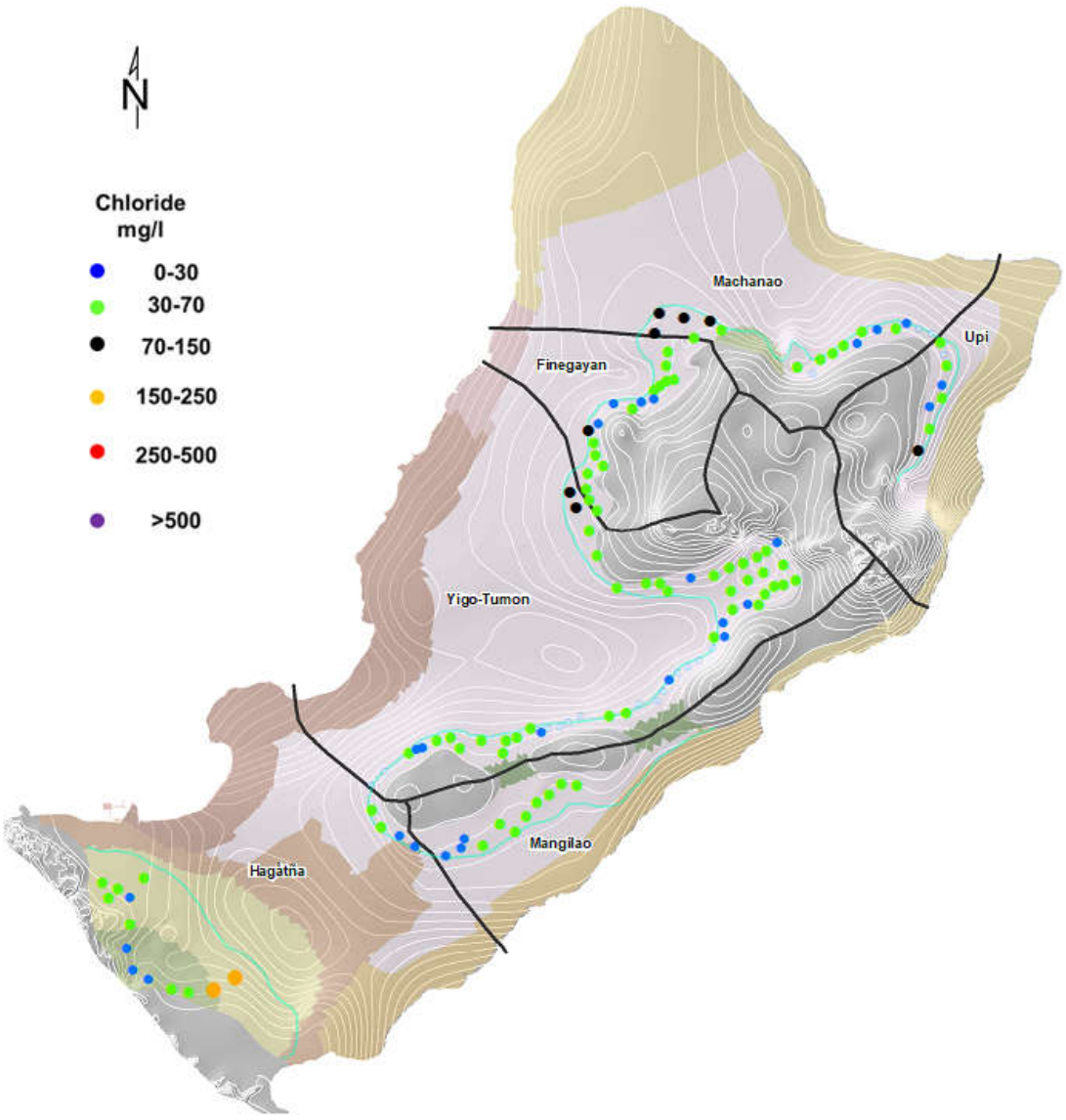

Fig. 4.7 200 gpm scenario NGLA chloride map.

Benchmark Count	<30 mg/L	Good	Standard	Marginal	Out of Standard	Threatened
	44	76	8	2	0	0

Basin	No. of Wells	Total Pump Rate (GPM)	Total Pump Rate (MGD)	Average Pump Rate (GPM)	Weighted Average [Cl-] (mg/L)
Machanao	17	3400	5	200	49
Upi	8	1600	2	200	50
Finegayan	20	4000	6	200	37
Yigo-Tumon	57	11400	16	200	37
Mangilao	11	2200	3	200	34
Hagåtña	17	3400	5	200	51
NGLA	130	26000	37	200	41

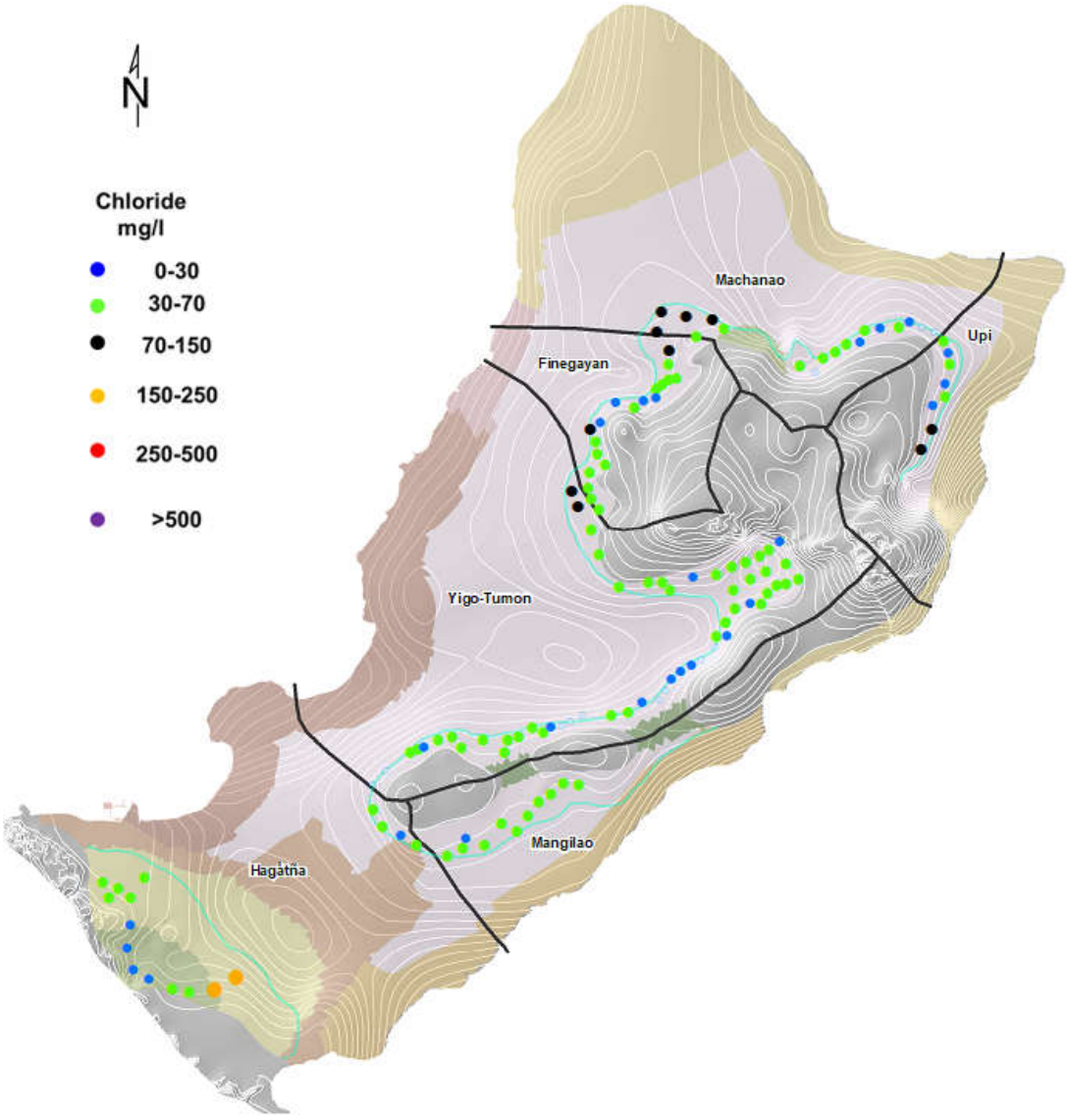

Fig. 4.8 225 gpm scenario NGLA chloride map.

Benchmark Count	<30 mg/L	Good	Standard	Marginal	Out of Standard	Threatened
	38	80	10	2	0	0

Basin	No. of Wells	Total Pump Rate (GPM)	Total Pump Rate (MGD)	Average Pump Rate (GPM)	Weighted Average [Cl-] (mg/L)
Machanao	17	3825	6	225	53
Upi	8	1800	3	225	52
Finegayan	20	4500	6	225	41
Yigo-Tumon	57	12825	18	225	40
Mangilao	11	2475	4	225	35
Hagåtña	17	3825	6	225	58
NGLA	130	29250	42	225	44

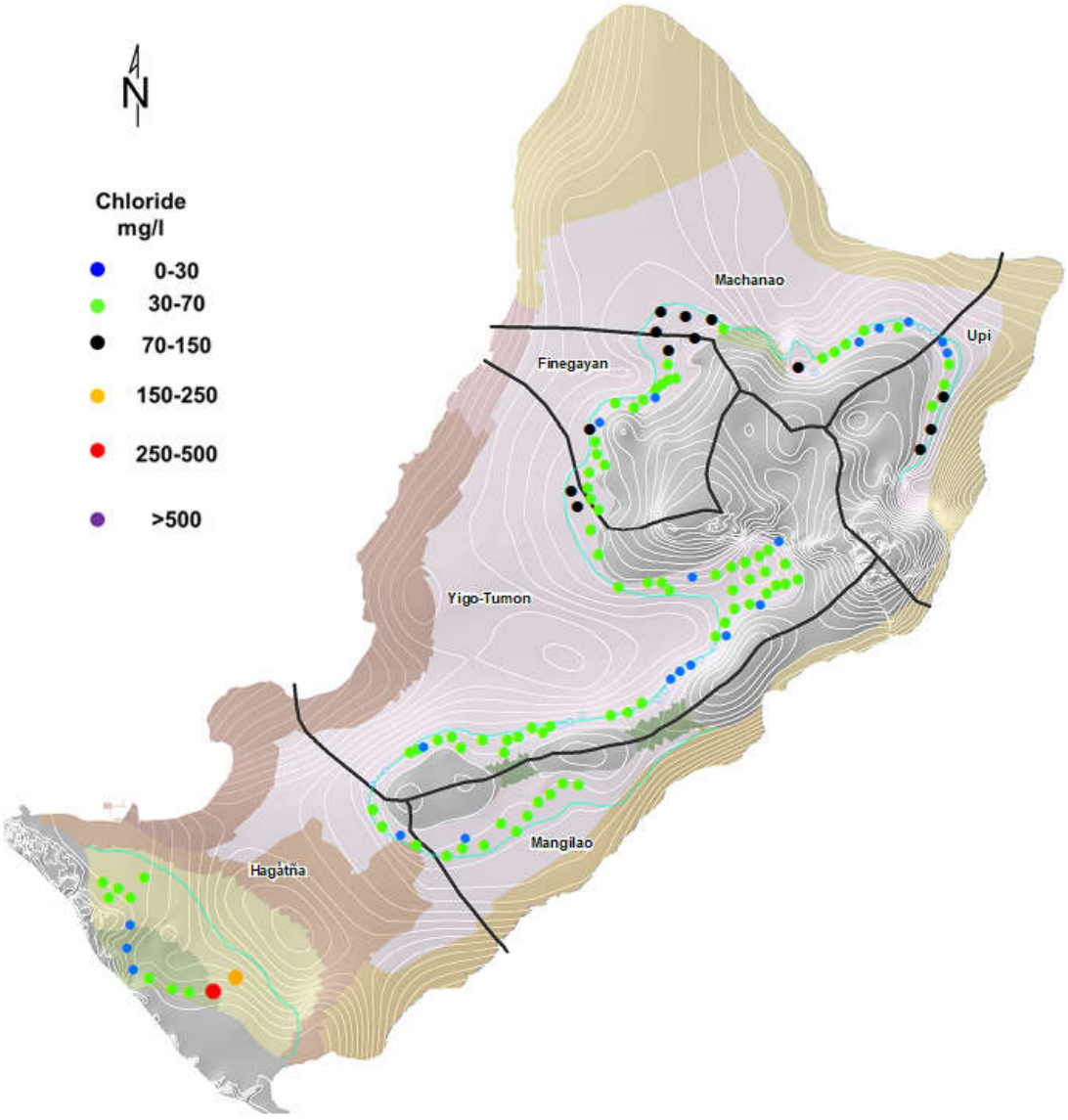

Fig. 4.9 250 gpm scenario NGLA chloride map.

Benchmark Count	<30 mg/L	Good	Standard	Marginal	Out of Standard	Threatened
	32	83	13	1	1	0

Basin	No. of Wells	Total Pump Rate (GPM)	Total Pump Rate (MGD)	Average Pump Rate (GPM)	Average [Cl-] (mg/L)
Machanao	17	4250	6	250	59
Upi	8	2000	3	250	58
Finegayan	20	5000	7	250	46
Yigo-Tumon	57	14250	21	250	44
Mangilao	11	2750	4	250	38
Hagåtña	17	4250	6	250	68
NGLA	130	32500	47	250	50

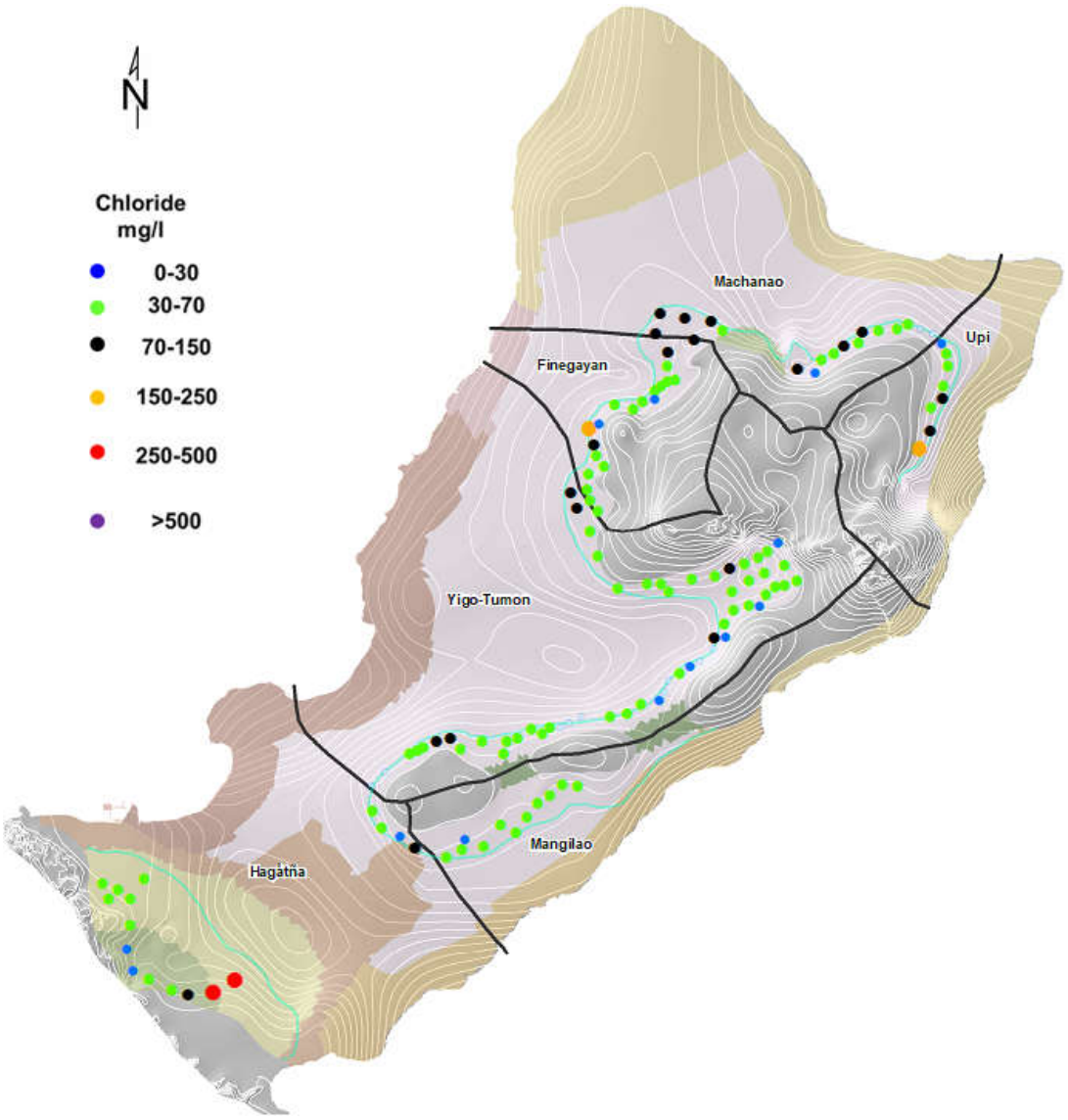

Fig. 4.10 275 gpm scenario NGLA chloride map.

Benchmark Count	<30 mg/L	Good	Standard	Marginal	Out of Standard	Threatened
	24	82	20	2	2	0

Basin	No. of Wells	Total Pump Rate (GPM)	Total Pump Rate (MGD)	Average Pump Rate (GPM)	Average [Cl-] (mg/L)
Machanao	17	4675	7	275	66
Upi	8	2200	3	275	68
Finegayan	20	5500	8	275	55
Yigo-Tumon	57	15675	23	275	50
Mangilao	11	3025	4	275	41
Hagåtña	17	4675	7	275	78
NGLA	130	35750	51	275	57

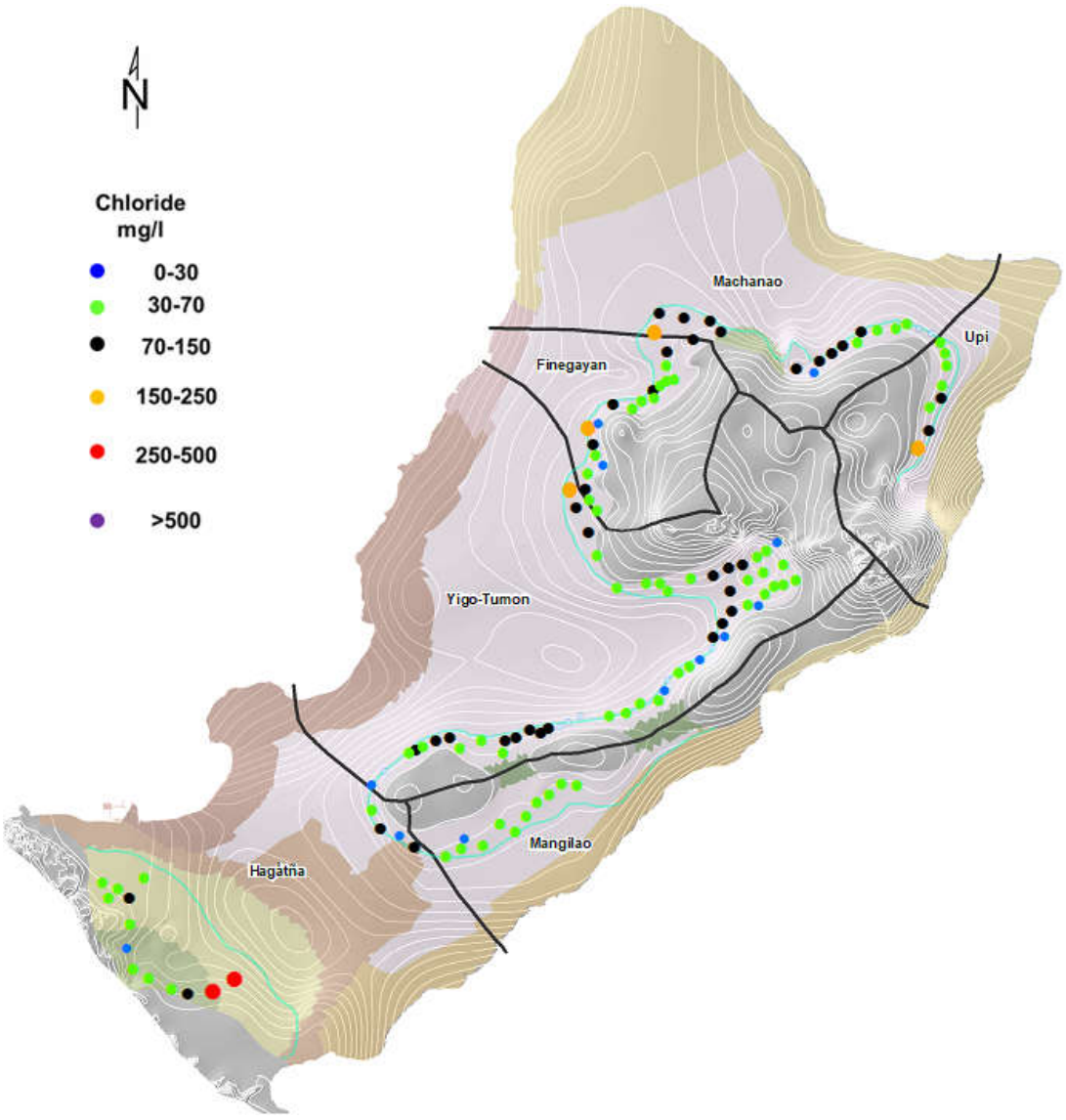

Fig. 4.11 300 gpm scenario NGLA chloride map.

Benchmark Count	<30 mg/L	Good	Standard	Marginal	Out of Standard	Threatened
	20	66	38	4	2	0

Basin	No. of Wells	Total Pump Rate (GPM)	Total Pump Rate (MGD)	Average Pump Rate (GPM)	Average [Cl-] (mg/L)
Machanao	17	5100	7	300	76
Upi	8	2400	3	300	83
Finegayan	20	6000	9	300	68
Yigo-Tumon	57	17100	25	300	58
Mangilao	11	3300	5	300	46
Hagåtña	17	5100	7	300	91
NGLA	130	39000	56	300	67

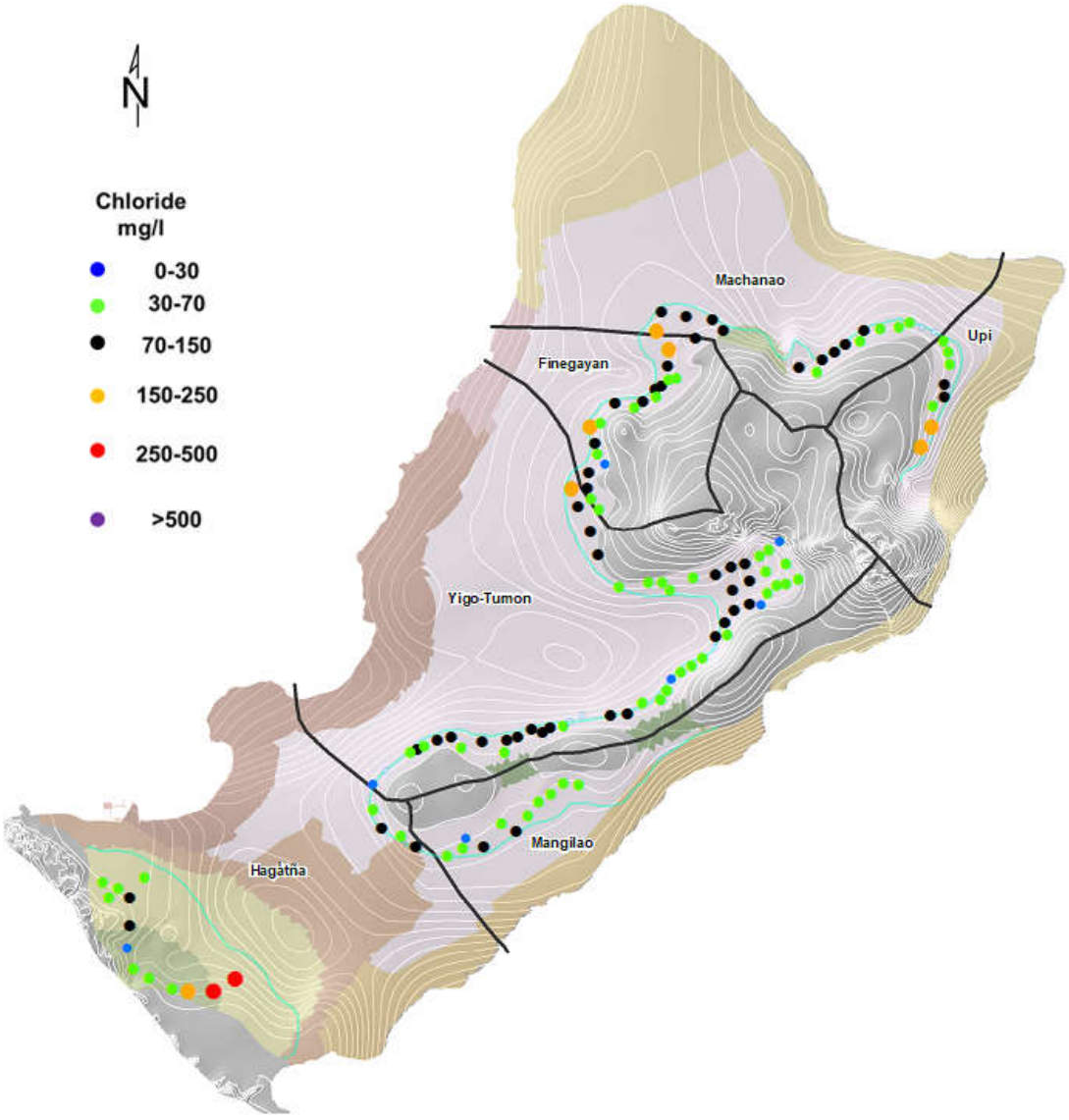

Fig. 4.12 325 gpm scenario NGLA chloride map.

Benchmark Count	<30 mg/L	Good	Standard	Marginal	Out of Standard	Threatened
	13	59	49	7	2	0

Basin	No. of Wells	Total Pump Rate (GPM)	Total Pump Rate (MGD)	Average Pump Rate (GPM)	Average [Cl-] (mg/L)
Machanao	17	5525	8	325	86
Upi	8	2600	4	325	100
Finegayan	20	6500	9	325	84
Yigo-Tumon	57	18525	27	325	70
Mangilao	11	3575	5	325	52
Hagåtña	17	5525	8	325	107
NGLA	130	42250	61	325	80

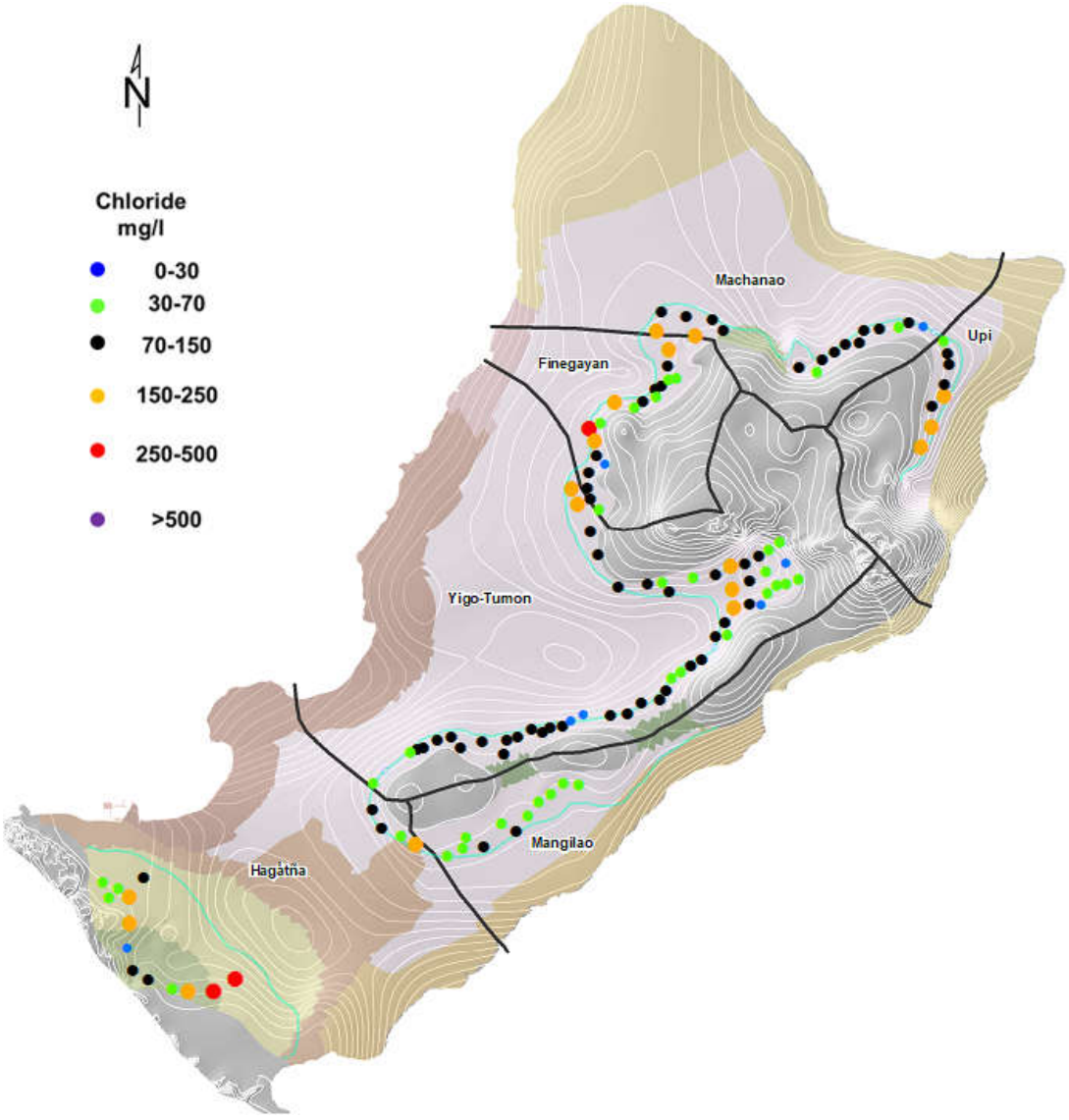

Fig. 4.13 350 gpm scenario NGLA chloride map.

Benchmark Count	<30 mg/L	Good	Standard	Marginal	Out of Standard	Threatened
	10	37	63	17	3	0

Basin	No. of Wells	Total Pump Rate (GPM)	Total Pump Rate (MGD)	Average Pump Rate (GPM)	Average [Cl-] (mg/L)
Machanao	17	5950	9	350	99
Upi	8	2800	4	350	119
Finegayan	20	7000	10	350	106
Yigo-Tumon	57	19950	29	350	86
Mangilao	11	3850	6	350	60
Hagåtña	17	5950	9	350	131
NGLA	130	45500	66	350	97

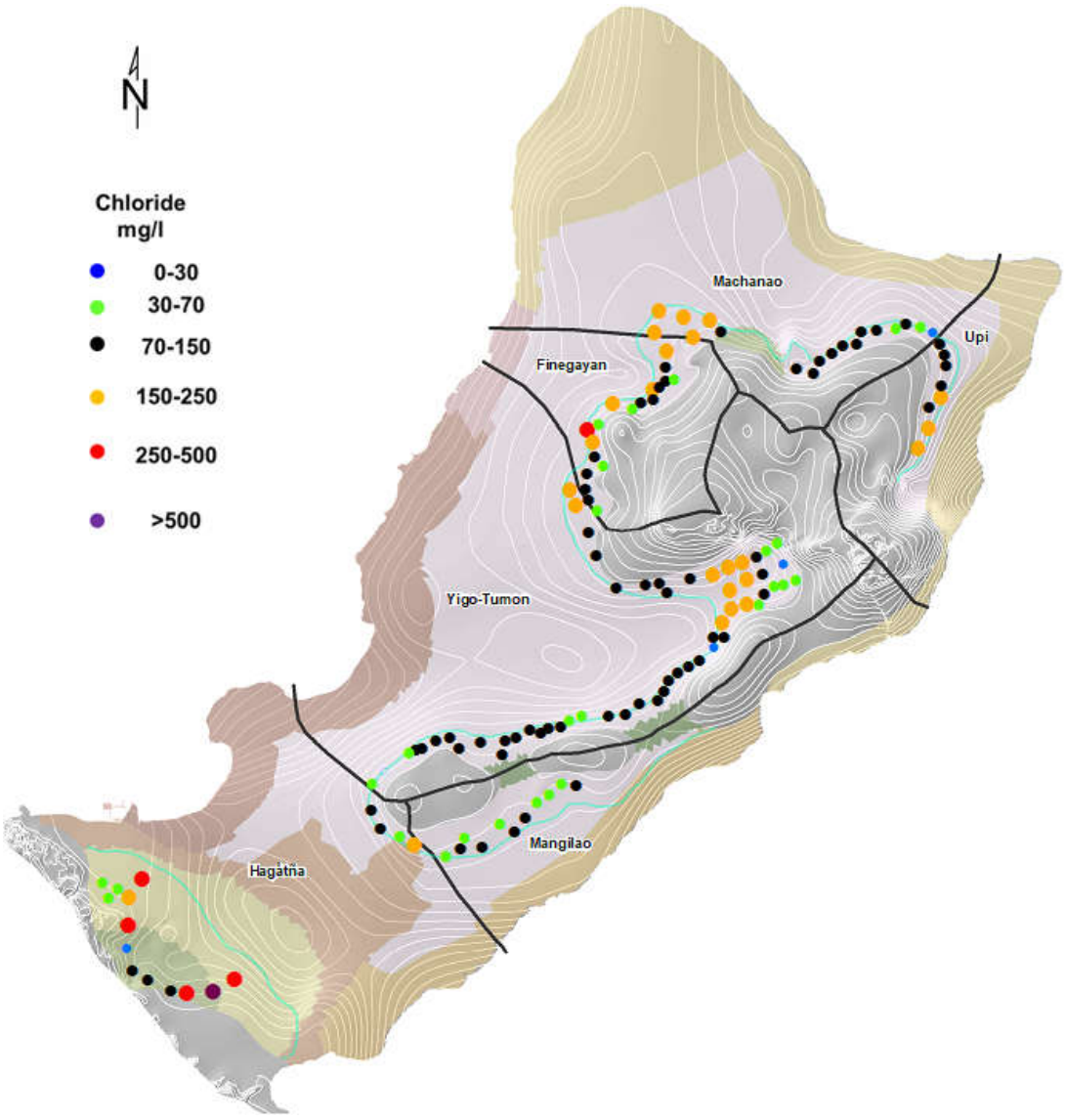

Fig. 4.14 375 gpm scenario NGLA chloride map.

Benchmark Count	<30 mg/L	Good	Standard	Marginal	Out of Standard	Threatened
	5	27	68	24	5	1

Basin	No. of Wells	Total Pump Rate (GPM)	Total Pump Rate (MGD)	Average Pump Rate (GPM)	Average [Cl-] (mg/L)
Machanao	17	6375	9	375	113
Upi	8	3000	4	375	140
Finegayan	20	7500	11	375	133
Yigo-Tumon	57	21375	31	375	106
Mangilao	11	4125	6	375	69
Hagåtña	17	6375	9	375	164
NGLA	130	48750	70	375	119

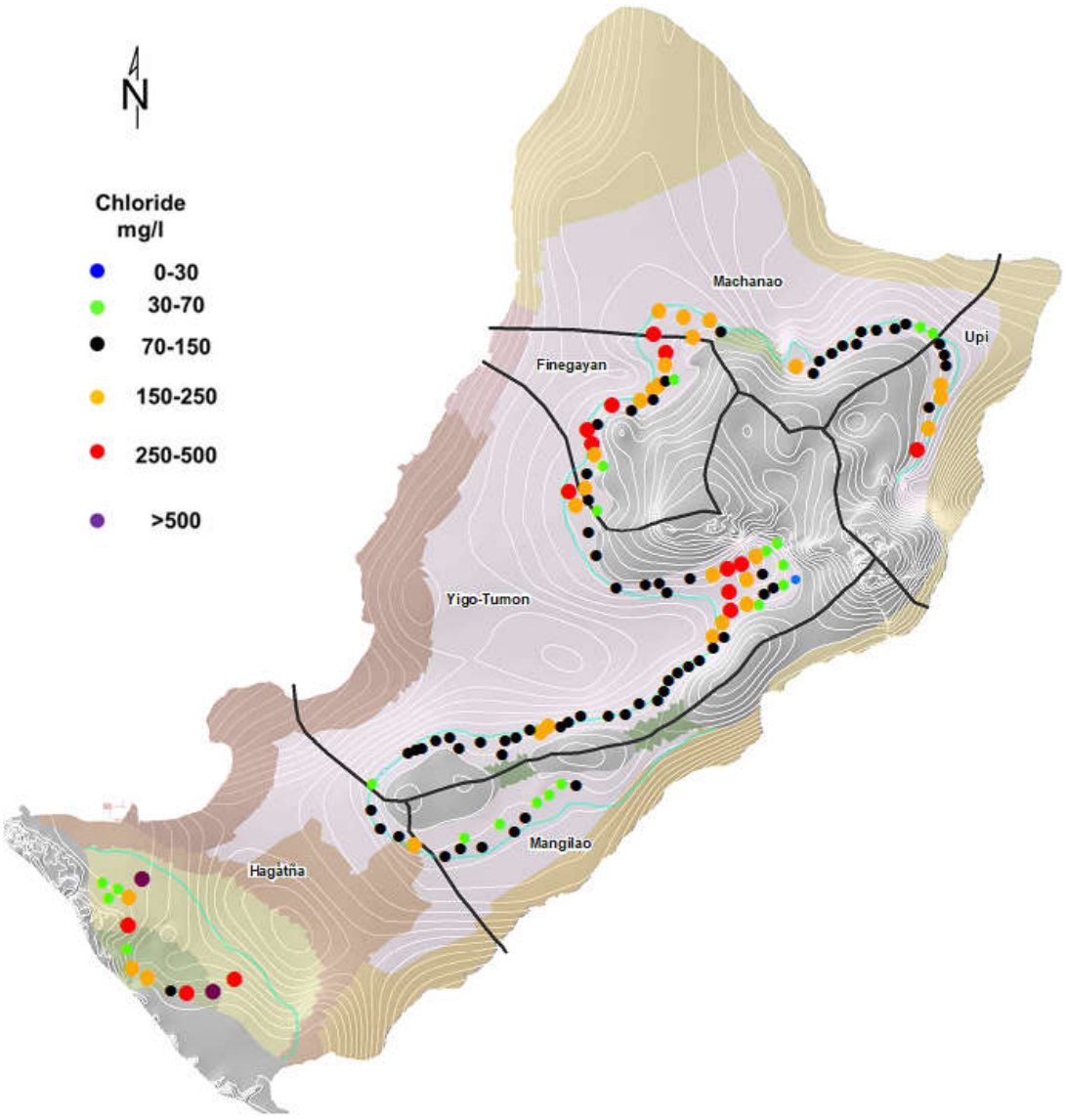

Fig. 4.15 400 gpm scenario NGLA chloride map.

Benchmark Count	<30 mg/L	Good	Standard	Marginal	Out of Standard	Threatened
	2	20	65	27	14	2

Basin	No. of Wells	Total Pump Rate (GPM)	Total Pump Rate (MGD)	Average Pump Rate (GPM)	Average [Cl-] (mg/L)
Machanao	17	6800	10	400	131
Upi	8	3200	5	400	163
Finegayan	20	8000	12	400	163
Yigo-Tumon	57	22800	33	400	131
Mangilao	11	4400	6	400	80
Hagåtña	17	6800	10	400	215
NGLA	130	52000	75	400	145

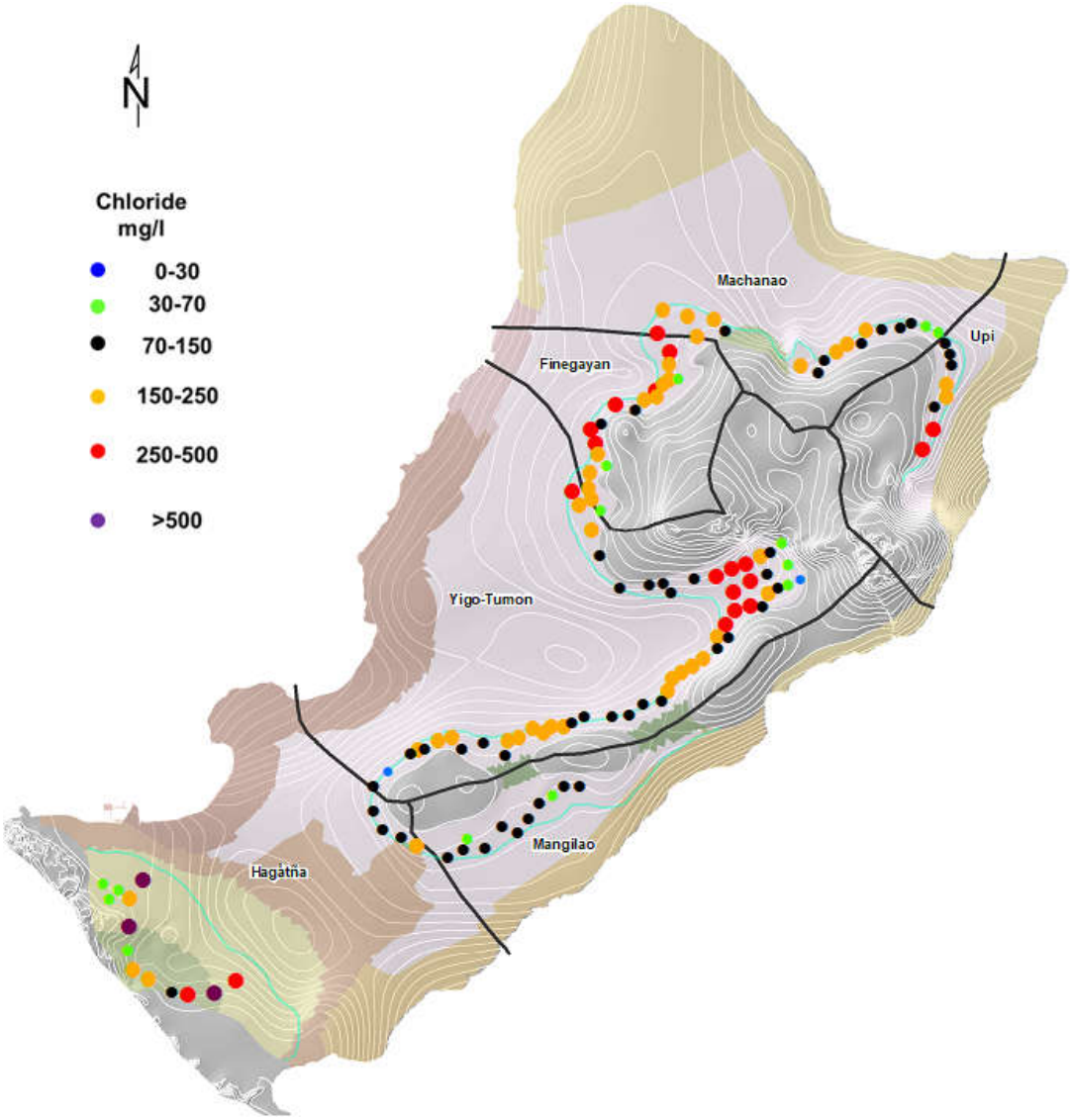

Fig. 4.16 425 gpm scenario NGLA chloride map.

Benchmark Count	<30 mg/L	Good	Standard	Marginal	Out of Standard	Threatened
	2	14	50	42	19	3

Basin	No. of Wells	Total Pump Rate (GPM)	Total Pump Rate (MGD)	Average Pump Rate (GPM)	Average [Cl-] (mg/L)
Machanao	17	7225	10	425	154
Upi	8	3400	5	425	188
Finegayan	20	8500	12	425	202
Yigo-Tumon	57	24225	33	425	162
Mangilao	11	4675	6	425	93
Hagåtña	17	7225	10	425	253
NGLA	130	55250	80	425	175

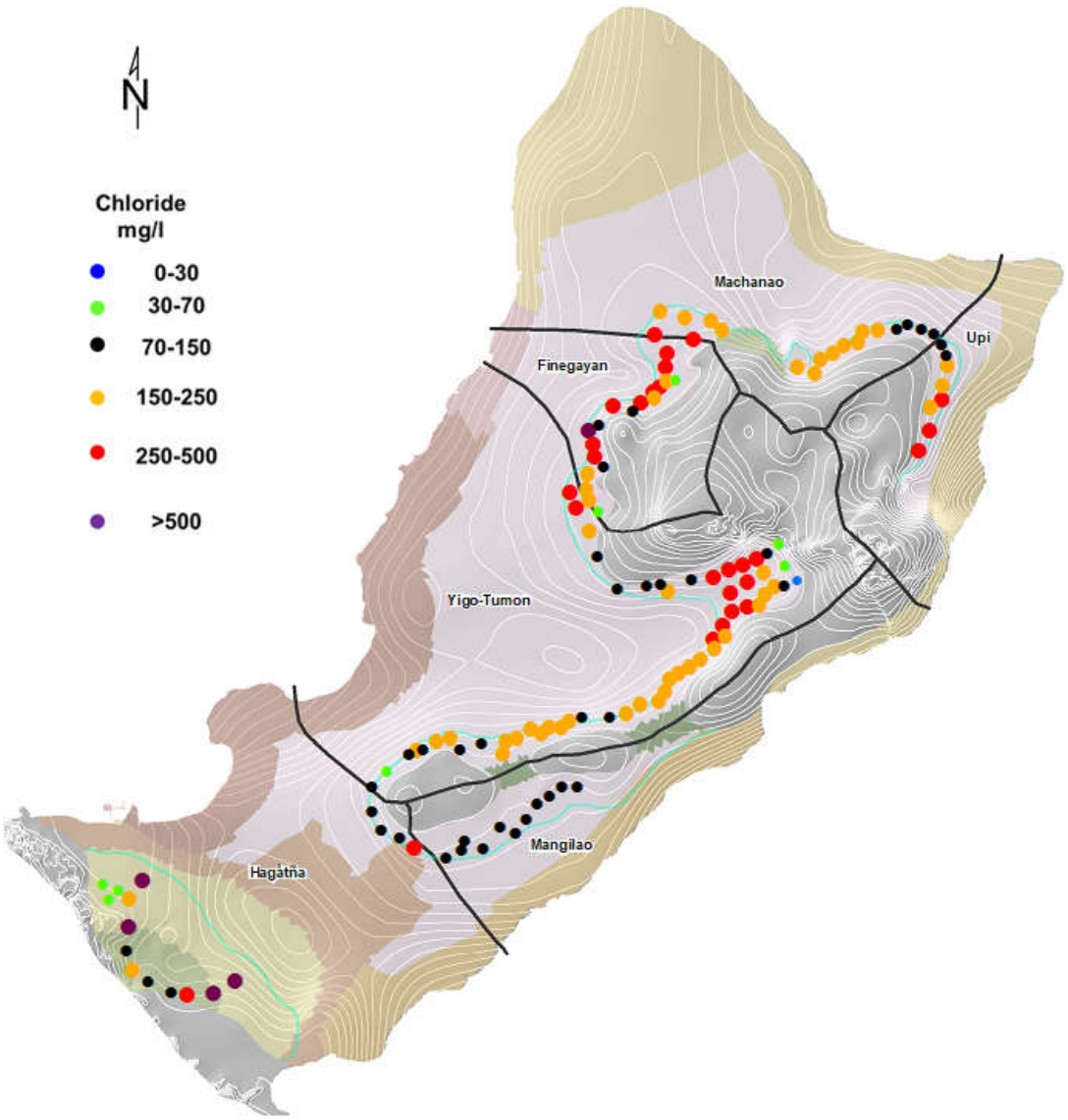

Fig. 4.17 450 gpm scenario NGLA chloride map.

Benchmark Count	<30 mg/L	Good	Standard	Marginal	Out of Standard	Threatened
	1	8	40	49	27	5

Basin	No. of Wells	Total Pump Rate (GPM)	Total Pump Rate (MGD)	Average Pump Rate (GPM)	Average [Cl-] (mg/L)
Machanao	17	7650	11	450	175
Upi	8	3600	5	450	213
Finegayan	20	9000	13	450	236
Yigo-Tumon	57	25650	37	450	198
Mangilao	11	4950	7	450	108
Hagåtña	17	7650	11	450	294
NGLA	130	58500	84	450	207

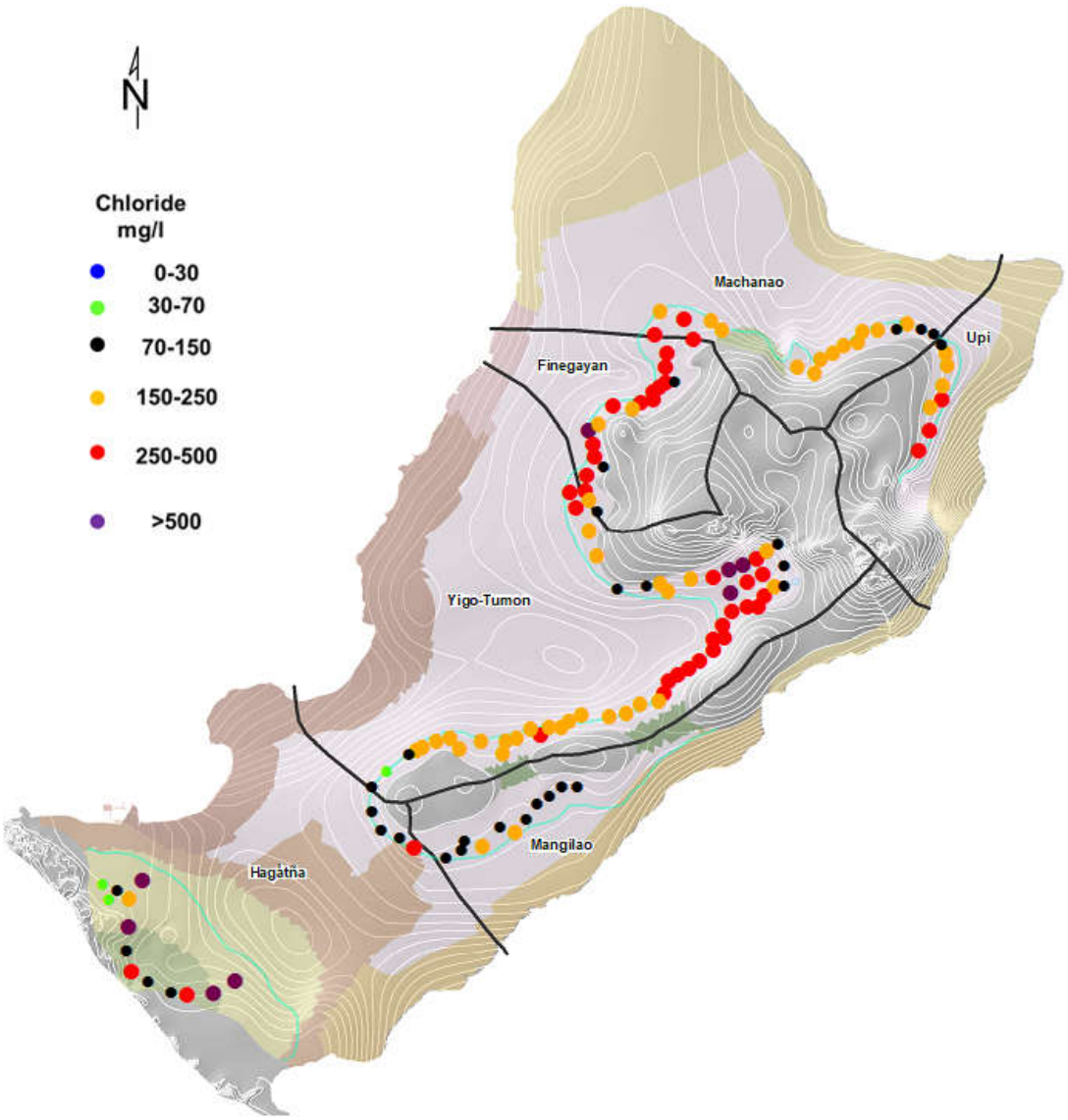

Fig. 4.18 475 gpm scenario NGLA chloride map.

Benchmark Count	<30 mg/L	Good	Standard	Marginal	Out of Standard	Threatened
	1	3	30	47	41	13

Basin	No. of Wells	Total Pump Rate (GPM)	Total Pump Rate (MGD)	Average Pump Rate (GPM)	Average [Cl-] (mg/L)
Machanao	17	8075	12	475	205
Upi	8	3800	5	475	242
Finegayan	20	9500	14	475	293
Yigo-Tumon	57	27075	39	475	243
Mangilao	11	5225	8	475	124
Hagåtña	17	8075	12	475	344
NGLA	130	61750	89	475	249

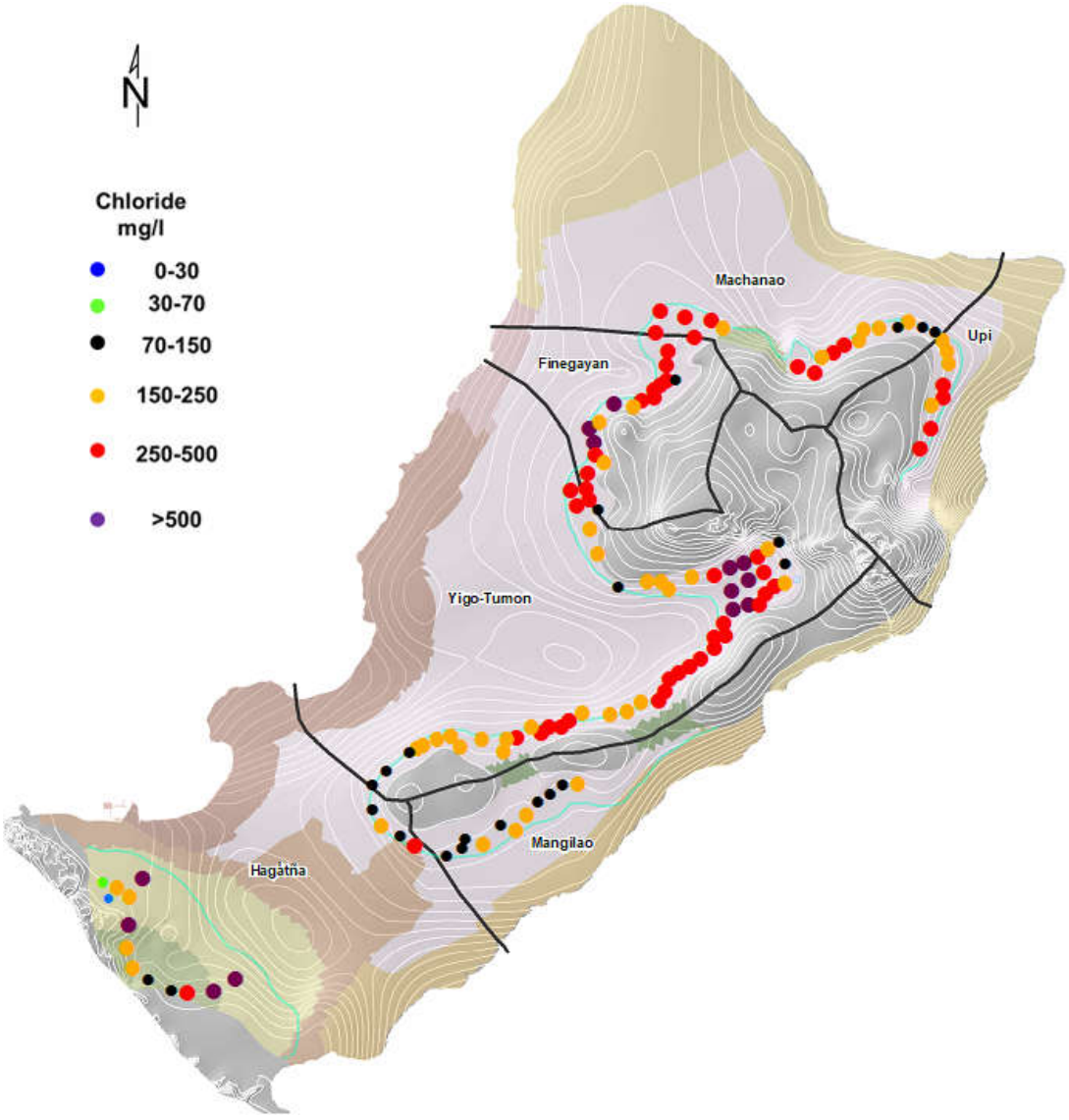

Fig. 4.19 500 gpm scenario NGLA chloride map.

Benchmark Count	<30 mg/L	Good	Standard	Marginal	Out of Standard	Threatened
	2	1	22	43	49	13

Basin	No. of Wells	Total Pump Rate (GPM)	Total Pump Rate (MGD)	Average Pump Rate (GPM)	Average [Cl-] (mg/L)
Machanao	17	8500	12	500	234
Upi	8	4000	6	500	272
Finegayan	20	10000	14	500	349
Yigo-Tumon	57	28500	41	500	294
Mangilao	11	5500	8	500	142
Hagåtña	17	8500	12	500	401
NGLA	130	65000	94	500	292

4.3.1 NGLA

The result of the NGLA model's pumping scenarios from 100-500 gpm, including the baseline scenario is shown on Fig. 4.20. Each modeled well is represented by a different colored line. Simulated weighted average chloride values under 30 mg/L for individual wells were omitted from the charts but included in composite concentration calculations. The *x*-axis is the pump rate (gpm) and on the *y*-axis is the simulated chloride concentration (mg/L). On the *y*-axis, at the 250mg/L mark is a horizontal red line that represents the GEPA secondary drinking water standard (US Environmental Protection Agency 2015). A thick black line is shown to represent the composite concentration for the NGLA, for each pumping scenario.

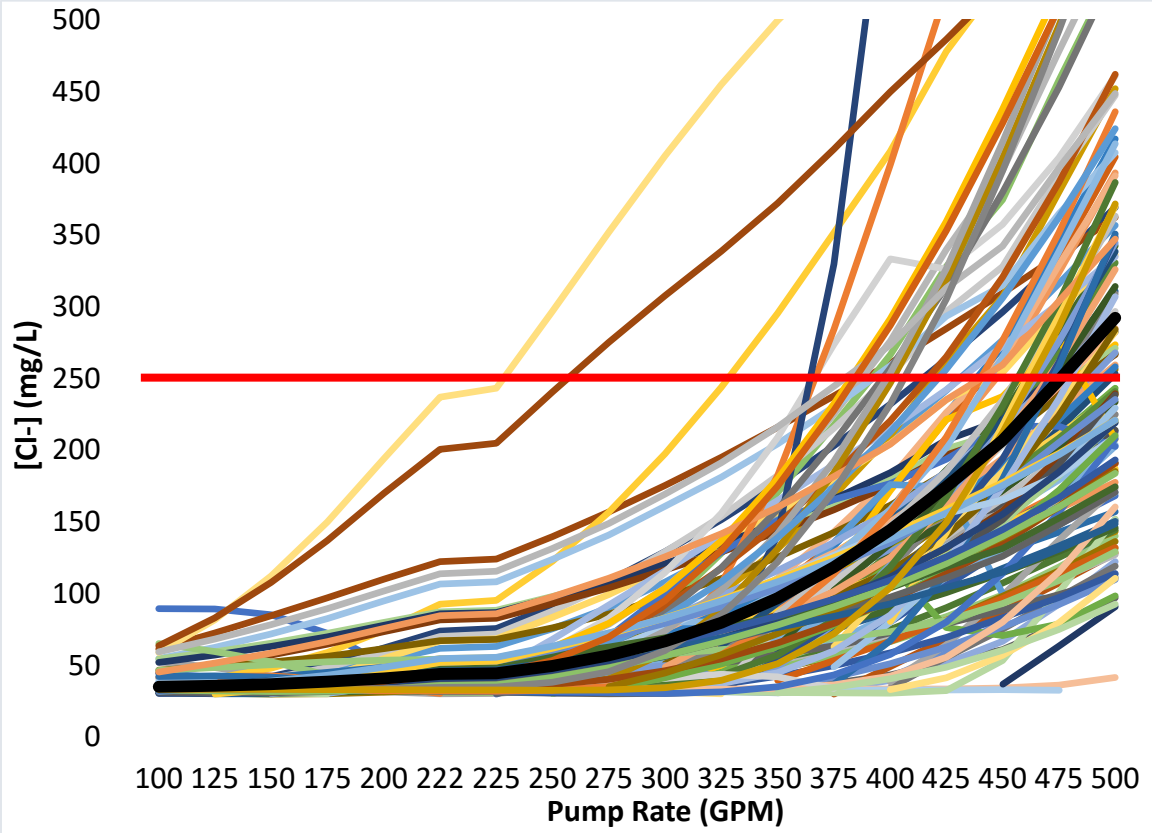

Fig. 4.20 NGLA, production vs chloride concentration. At 475 gpm, the composite concentration is 249 mg/L, which corresponds with 89 MGD of total withdrawal.

4.3.2 Per basin

Charts similar to the NGLA chart (Fig. 4.20) were produced for each basin (Fig. 4.21 - 4.26). Each chart has thick black line representing the composite concentration for the basin. All charts include a legend to help locate individual simulated parabasal wells (Fig. 3.1).

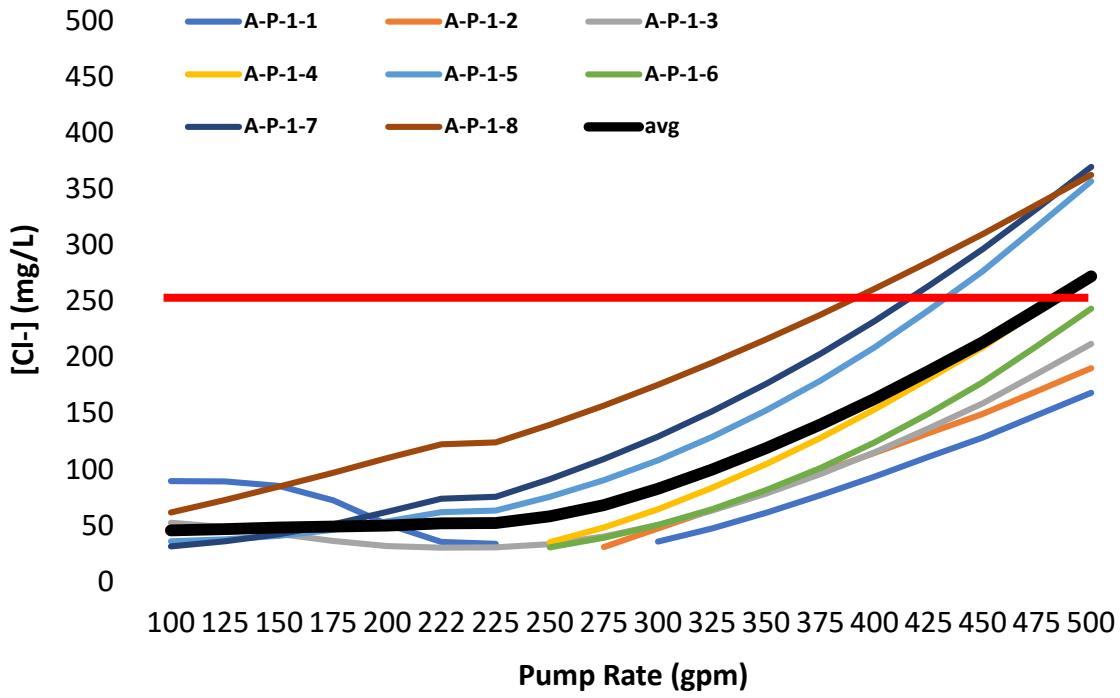

Fig. 4.21 Upi basin, production vs chloride.

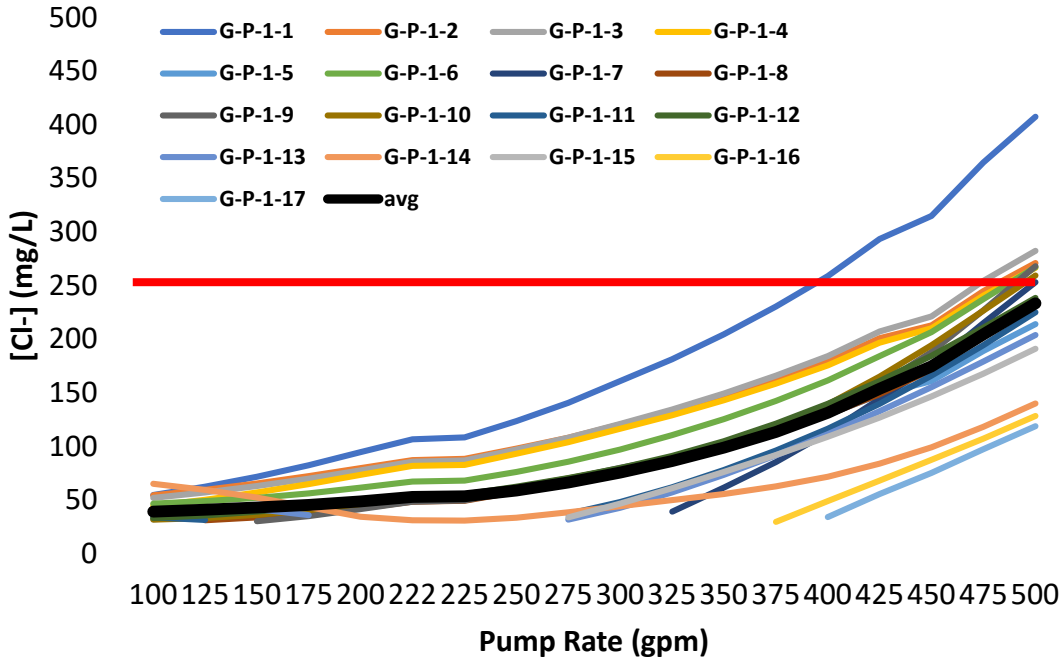

Fig. 4.22 Machanao basin, production vs chloride.

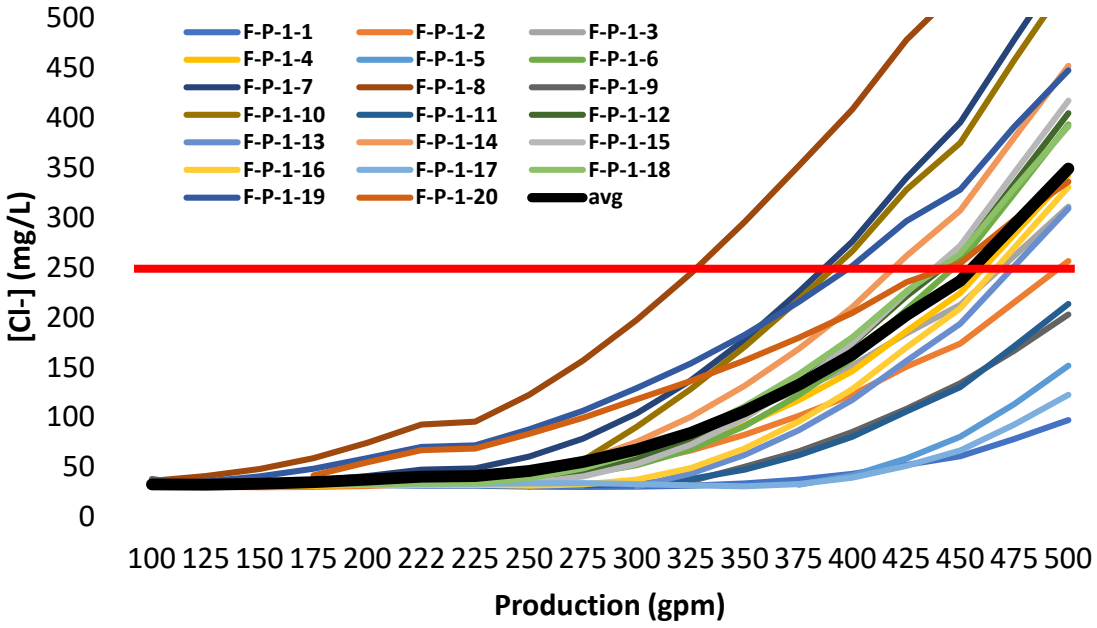

Fig. 4.23 Finegayan basin, production vs chloride.

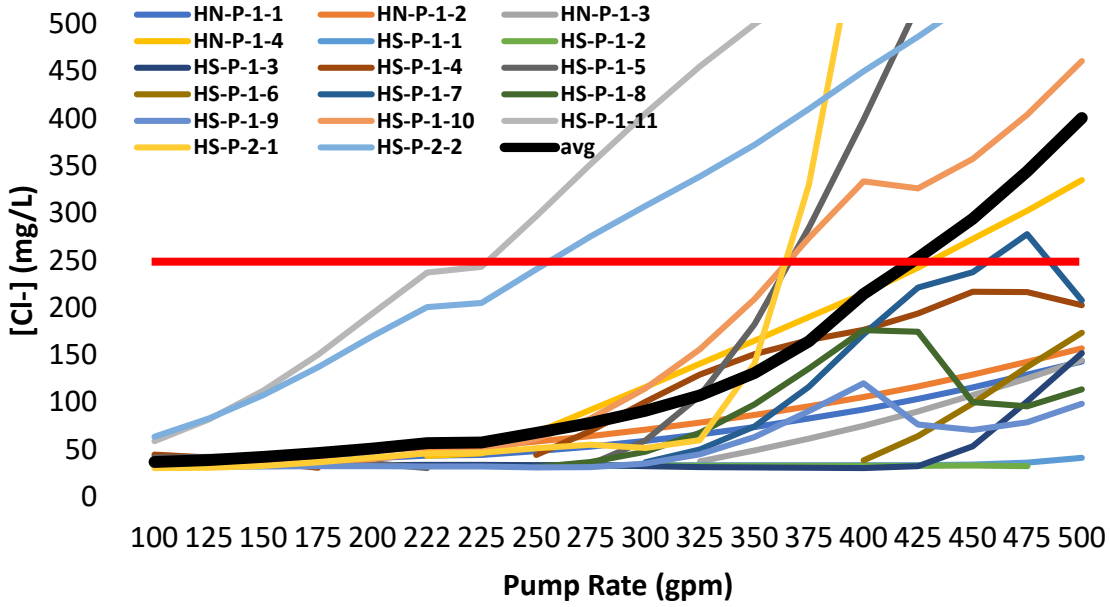

Fig. 4.24 Hagåtña basin production vs chloride.

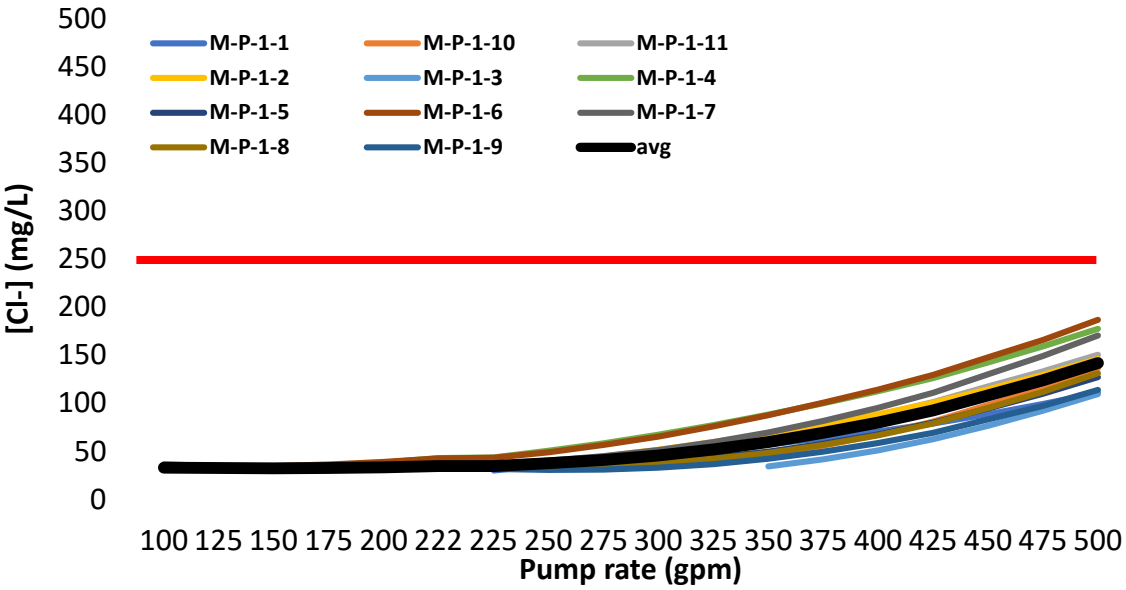

Fig. 4.25 Mangilao basin production vs chloride.

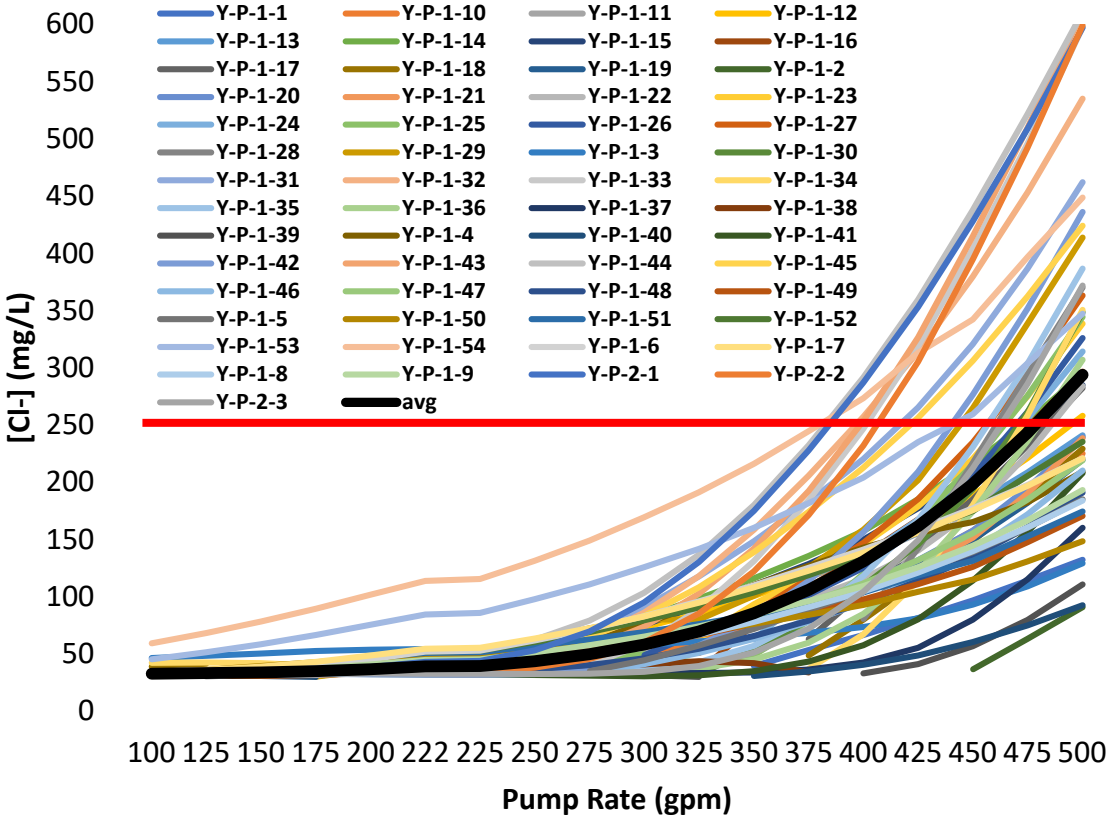

Fig. 4.26 Yigo-Tumon basin production vs chloride.

Chapter 5
DISCUSSION

5.1 Chart and Map interpretation

Results are discussed in terms of the graphs of chloride response to increased simulated pumping rates (Fig. 4.20-4.26) and spatial patterns (Fig. 4.1-4.19). The model data will be compared against the actual system data.

5.1.1 Upi basin

Eight wells were simulated in the Upi parabasal zone. This basin's parabasal zone produces freshwater with composite concentration less than 250 mg/L up to about 475 gpm in each well (Fig. 4.21), totaling about 5.5 MGD. The parabasal zone in this basin is the smallest in area. It is widest in the north and narrows toward the south. The Upi basin chart (Fig. 4.21) shows chloride concentration of the wells increasing with pump rate, almost parallel to the average but with a wide range. The maps (Fig. 4.3-4.19) show that the three southern Upi wells (A-P-1-8, A-P-1-7 and A-P-1-5) (Fig. 3.1) are most sensitive to pumping, exceeding 250 mg/L weighted average chloride concentration as pump rate approaches 475 gpm (Fig. 4.18). This increased sensitivity to pumping may be due to the wells being located nearest the no-pumping saltwater-toe (Gingerich 2013). The saltwater-toe may be migrating inland and could cause classical up-coning (Fig. 2.3) of saltwater into the wells. However, the limestone of the freshwater phreatic zone is karst thus the Darcian model may not accurately describe the phenomena.

Model results show that the Upi basin parabasal zone has potential for development but the hydrologic data from this basin are very sparse. More data will be needed for future modeling construction and calibration.

5.1.2 Machanao basin

Seventeen wells were simulated in the Machanao parabasal zone. This basin's parabasal zone produces freshwater with a composite concentration less than 250 mg/L up to about 500 gpm in each well (Fig. 4.22), totaling about 12.2 MGD. This basin's chart is comparable to the Upi basin chart (Fig. 4.21) where the trend of chloride concentrations with higher pumping rates are almost parallel to the average but with a wide range.

Simulated well G-P-1-1 (Fig. 3.1, 4.14, 4.22) is an outlier with the highest chloride levels in nearly all pumping scenarios and it is first to exceed 250 mg/L chloride concentration at 375 gpm. The increased sensitivity to pumping could be due to it being located down-gradient to simulated wells F-P-1-20 and F-P-1-19. A few other simulated wells exceed the secondary standard around 475-500 gpm.

Chloride maps (Fig. 4.14-4.19) show that simulated wells exceed 250 mg/L weighted average chloride concentration starting in the west with G-P-1-1 after 375 gpm and then migrates westward to G-P-1-10 at 500 gpm. Similar to the Upi basin, the eastern section of the Machanao basin is also very sparse in hydrologic data.

At the uniform pump rate of 222 gpm, the basin has a similar composite concentration to the actual system while producing an additional 4 MGD with 12 more production wells (Fig. 4.1-4.2). The actual basin has two production wells in the parabasal zone, AG-1 and AG-2a. AG-1 has production and salinity values similar to the simulated Machanao wells but with a well depth of -27 feet below msl. AG-2a is an exceptional well,

producing over 500 gpm at -81.2 ft well bottom elevation but with an average chloride concentration of 37 mg/L (Simard et al. 2015). Simulated well G-P-1-3 is the closest well in the Machanao basin that corresponds to the location of actual well AG-2a, but is sited closer to the saltwater toe.

5.1.3 Finegayan basin

Twenty wells were simulated in the Finegayan parabasal zone. This basin's parabasal zone produces freshwater with composite concentration less than 250 mg/L up to about 450 gpm per well for a total of about 13 MGD (Fig. 4.23). Simulated salinities from the Finegayan parabasal 222 gpm scenario are comparable to those from the actual Finegayan parabasal wells which exhibited "Exceptional" to "Standard" quality chloride concentrations (Simard et al. 2015) (Fig. 4.1). Baseline results improved chloride quality about 67% from "Standard" to "Good" quality while producing one more MGD over the observed basin with two additional wells.

High simulated chloride values at F-P-1-8 and F-P-1-19 show that the simulated saltwater toe could have migrated inland causing the higher chloride values (Fig. 4.3-4.19). The location of simulated well F-P-1-8 closely corresponds to well F-13 in the actual system, a basal well with average chloride concentration exceeding the GEPA recommendation of 250 mg/L. F-13 could be hydrologically connected to a fault near Haputo Bay, an area with a high hydraulic conductivity and the highest simulated coastal discharge (Gingerich 2013). The underlying seawater may be recirculating through conduits hydrologically connected to faults in the area. This may explain why F-P-1-8 has a much higher weighted average chloride concentration at every pumping scenario compared to other wells simulated in the Finegayan basin.

5.1.4 Hagåtña basin

Seventeen wells were simulated in the Hagåtña parabasal, compared to 27 in the observed system. This basin's parabasal zone produces freshwater with composite concentration less than 250 mg/L up to about 450 gpm per well for a total of about 11 MGD (Fig. 4.24). Simulated salinities in the basin model results (Fig. 4.3-4.19) show that the Hagåtña parabasal can be divided into three sectors, which show different response: northern parabasal near the Barrigada Rise, southwest parabasal, and the southeast parabasal, the latter two of which form on the footwall of the Pago-Adelup fault.

Simulated chloride concentrations from the baseline scenario's Hagåtña parabasal (Fig. 4.1) are similar to the actual Hagåtña parabasal wells (Fig. 4.2) where southwest wells were typically in the "Exceptional" to "Good" chloride concentration benchmark. Two southwest wells, HS-P-2-1 and HS-P-1-5 exhibit "Marginal" quality production at the baseline scenario and are the first to exceed the 250 mg/L standard. This high chloride is typical of wells, even parabasal wells, located on the southwest end of Hagåtña basin (Fig. 4.2).

In the northern Hagåtña parabasal zone, simulated wells performed better than NAS-1 in the actual system at 250 gpm (Fig. 4.9, 4.17), with weighted average chloride concentrations in the "Good" range compared to the "Standard" quality shown in the map of the actual system (Fig. 4.2). The lower simulated chloride values are likely due to the shallower simulated well bottom depth of -40 ft below msl compared to the actual well -60 ft below msl bottom depth of NAS-1. After 450 gpm, HN-P-1-4 was the only

northern Hagåtña well to exceed 250 mg/L chloride concentration likely due to it being in an area of higher regional hydraulic conductivity.

5.1.5 Mangilao basin

Eleven wells are simulated in the Mangilao Basin's parabasal zone. This basin's parabasal zone produces freshwater with a composite concentration less than 250 mg/L up to about 500 gpm per well for a total of about 8 MGD (Fig. 4.24). The actual system has eight wells located in the parabasal zone. The chloride level for each well is nearly equal to the average until pumping rate reaches about 250 gpm (Fig. 4.25). The production weighted average chloride concentration does not intersect with the 250 mg/L standard even at the final pumping scenario of 500 gpm. From 250 gpm to 500 gpm, the deviation from the average is relatively small compared to the other basins. At 500 gpm, the chloride level for each well is still less than 200 mg/L. The maps (Fig. 4.3-4.19) show that when pump rate increases to 475 gpm, wells nearest the saltwater toe, M-P-1-4 and M-P-1-6, are first to reach the 150-250 mg/L chloride concentration range.

At the uniform pump rate of 222 gpm, the basin's composite concentration was improved by about 67% at 35 mg/L compared to the actual basin's average, at 105 mg/L while doubling the volume of produced freshwater (Fig. 4.1-4.2).

5.1.6 Yigo-Tumon basin

Fifty-seven wells are simulated in the Yigo-Tumon parabasal zone—five fewer wells than the actual system. This basin's parabasal zone produces freshwater with a composite concentration less than 250 mg/L up to about 475 gpm per well for a total of about 39 MGD (Fig. 4.24). Apart from wells Y-P-2-2 and Y-P-1-53, there is little deviation from the average chloride from 100 gpm up to 250 gpm (20.5 MGD) (Fig. 4.26). After 250 gpm, deviation from the average fans out, and spreads wide similarly to the Finegayan basin chart. All wells maintain chloride concentrations below 250 mg/L until after 375 gpm (Fig. 4.2-4.19).

At the uniform pump rate of 222 gpm, the basin's composite concentration was improved by about 60% at 39 mg/L compared to the actual system's average, at 98 mg/L. Another factor contributing to the lower overall salinity levels seen in the model is the lower overall total withdrawal from the basin. The numerical model withdraws about 3 MGD less freshwater. Model results for the Yigo-Tumon basin show that even if all basal zone wells could be moved into the parabasal zone, the freshwater production would need to be supplemented via the adjacent basins.

Saltwater encroachment is visible in the basin; as pump rate increases from 300-500 gpm (Fig. 4.2-4.19). It is possible that simulated wells located in the Yigo-trough are pulling the saltwater toe inland, closer to the volcanic contact.

Chapter 6
CONCLUSION

This project provides water resource managers with sustainable management criteria for Guam's aquifer. The numerical model results further suggest that parabasal wells will reduce the risk of saltwater intrusion and further increase the aquifer production capacity. This may bolster the previous studies that recommended parabasal development (McDonald and Jenson 2003) and (Simard et al 2015), showing existing parabasal wells had lower salinity than basal wells. Baseline simulation results (Fig. 4.2) produced 42 MGD (130 parabasal zone wells) with a composite concentration (Gingerich 2019) (an overall volume weighted-average chloride concentration) of 44 mg/L compared to the actual system (Fig. 4.1) that produced 39 MGD (73 basal zone wells, 48 parabasal zone wells) with a composite concentration of 123 mg/L. However, 30% of baseline simulation wells resulted in anomalous concentrations possibly due to roundoff or truncation error.

The modeled parabasal system can produce up to 89 MGD (Fig. 4.18) while maintaining the composite concentration at or below 250 mg/L. However, 54 simulated wells showed chloride concentrations at 250 mg/L or greater.

Model results also show that the Finegayan and Hagåtña basins have the greatest potential for water quality improvement with simulated weighted average chloride concentrations about three and two times less, respectively, than the observed basin averages. Total production for the Yigo-Tumon and Hagåtña was reduced from the observed system by about three and four MGD respectively. The distribution system will need to be redesigned to allow the other basins to make up for the reduced production.

To achieve a lower overall salinity, output in the most productive basins, Yigo-Tumon and Hagåtña, would need to be reduced. To make up for the lower output, other basins could be developed further and delivery system efficiency must be improved. Now water managers have the confidence to determine future well development and realize a better production well configuration. Also, rather than rehabilitating old and poor performing wells, this study recommends abandoning those wells and consider drilling at a better location, the parabasal zone.

REFERENCES

Ayers JF, Clayshulte RN (1984) A preliminary study of the hydrogeology of northern Guam. University of Guam Technical report 56, Water and Energy Research Institute of the Western Pacific, Univ. of Guam, Mangilao, Guam

Beal LK, Wong CI, Bautista KK, et al (2019) Isotopic and geochemical assessment of the sensitivity of groundwater resources of Guam, Mariana Islands, to intra- and inter-annual variations in hydroclimate. Journal of Hydrology 568:174–183. https://doi.org/10.1016/j.jhydrol.2018.10.049

Bendixson VM, Jenson JW, Habana NC (2013) The Northern Guam Lens Aquifer Database. University of Guam Technical report 141, Water and Environmental Research Institute of the Western Pacific, Univ. of Guam, Mangilao, Guam

Camp Dresser and McKee Inc. (1982) Northern Guam Lens Study, Groundwater Management Program, Aquifer Yield report, Final report, Guam Environmental Protection Agency, Barrigada, Guam

Contractor DN (1983) Numerical modeling of saltwater intrusion in the Northern Guam Lens. J Am Water Resources Assoc 19:745–751. https://doi.org/10.1111/j.1752-1688.1983.tb02797.x

Contractor DN, Srivastava R (1990) Simulation of saltwater intrusion in the Northern Guam Lens using a microcomputer. Journal of Hydrology 118:87–106. https://doi.org/10.1016/0022-1694(90)90252-S

Ford D, Williams P (2007) Karst Hydrogeology and Geomorphology: Ford/Karst Hydrogeology and Geomorphology. John Wiley & Sons Ltd,., West Sussex, England

Gingerich SB (2013) The effects of withdrawals and drought on groundwater availability in the Northern Guam Lens Aquifer, Guam. US Geol Surv Sci Invest Rep 2013-5216

Gingerich SB, Jenson JW (2010) Groundwater availability study for Guam; goals, approach, products, and schedule of activities. US Geol Surv Fact Sheet 2010–3084

Gingerich SB, Johnson AG, Rosa SN, et al (2019) Water Resources on Guam--Potential Impacts of and Adaptive Response to Climate Change. US Geol Surv Sci Invest Rep 2019-5095

Guam Visitor's Bureau (2018) 2018 GVB annual report. https://www.guamvisitorsbureau.com/reports/annual-report. Accessed 17 Feb 2020

Jocson JMU, Jenson JW, Contractor DN (2002) Recharge and aquifer response: Northern Guam Lens Aquifer, Guam, Mariana Islands. J Hydrol 260:231–254. https://doi.org/10.1016/S0022-1694(01)00617-5

Johnson AG (2012) A water-budget model and estimates of groundwater recharge for Guam. US Geol Surv Sci Invest Rep 2012–5028

Joint Guam Program Office (2010) Relocating marines from Okinawa: visiting aircraft carrier Berthing, and Army Air and Missile Defense Task Force. In: Guam Program Management Office (ed) Final environmental impact statement: Guam and CNMI military relocation. Naval Facilities Engineering Command, Pacific 322

Joshua I. Tracey Jr., Seymour O. Schlanger, John T. Stark, et al (1964) General geology of Guam. US Geol Surv Prof Pap 403-A

McDonald MQ, Jenson JW (2003) Chloride History and Trends of Water Production Wells in the Northern Guam Lens Aquifer. University of Guam Technical report 98, Water and Environmental Research Institute of the Western Pacific, Univ. of Guam, Mangilao, Guam

Military Installations (2020) Joint Region Marianas - Naval base Guam installation booklet in-depth overview. https://installations.militaryonesource.mil/installation-booklet/joint-region-marianas-naval-base-guam. Accessed 17 Feb 2020

Mink JF (1992) Groundwater in Northern Guam Sustainable Yield and Ground Water Development. Barrett Consulting Group Final Engineering report, Agana, Guam

Mink JF, Vacher HL (2004) Hydrogeology of northern Guam. In: Quinn T (ed) Developments in sedimentology. Elsevier, Amsterdam, pp 743–761

Mylroie JL, Jenson JW, Jocson JMU (1999) Karst Geology and Hydrology of Guam: A Preliminary Report. University of Guam Technical report 89, Water and Environmental Research Institute of the Western Pacific, Univ. of Guam, Mangilao, Guam

Partin JW, Jenson JW, Banner JL, et al (2012) Relationship between modern rainfall variability, cave dripwater, and stalagmite geochemistry in Guam, USA: RAINFALL AND STALAGMITE GEOCHEMISTRY, GUAM. Geochem Geophys Geosyst 13:n/a-n/a. https://doi.org/10.1029/2011GC003930

Pilson MEQ (2013) An introduction to the chemistry of the sea, Second edition. Cambridge University Press, Cambridge

Rotzoll K, Gingerich SB, Jenson JW, El-Kadi AI (2013) Estimating hydraulic properties from tidal attenuation in the Northern Guam Lens Aquifer, territory of Guam, USA. Hydrogeol J 21:643–654. https://doi.org/10.1007/s10040-012-0949-9

Siegrist HG, Reagan MK (2008) Geologic Map and Sections of Guam, Mariana Islands. Revision of original map from USGS Professional Report 403A (1964) by Tracey JI, Jr., Schlanger SO, Stark JT, Doan DB, May HG. Field interpretations for 2008 revision assisted by Randall RH and Jenson JW. Water and Environmental Research Institute of the Western Pacific, University of Guam, Mangilao, Guam

Simard CA, Jenson JW, Lander MA, et al (2015) Salinity in the Northern Guam Lens Aquifer. University of Guam Technical report 143, Water and Environmental Research Institute of the Western Pacific, Univ. of Guam, Mangilao, Guam

US Environmental Protection Agency (1978) Guam: sole or principal source aquifer designation. Federal Register 43 FR 17888, 26 April 1978

US Environmental Protection Agency (2015) Water Quality Standards Regulations: Guam. https://www.epa.gov/wqs-tech/water-quality-standards-regulations-guam. Accessed 17 Feb 2020

Vann DT, Bendixson VM, Roff DF, et al (2014) Topography of the Basement Rock Beneath the Northern Guam Lens Aquifer and Its Implications for Groundwater Exploration and Development. University of Guam Technical report 142, Water and Environmental Research Institute of the Western Pacific, Univ. of Guam, Mangilao, Guam

Voss CI, Provost AM (2002) SUTRA, a model for saturated-unsaturated variable-density ground-water flow with solute or energy transport. US Geol Surv Water Resour Invest 02– 4231

Ward PE, Hoffard SH, Davis DA (1965) Hydrology of Guam. US Geol Surv Prof Pap 403-H

APPENDICES

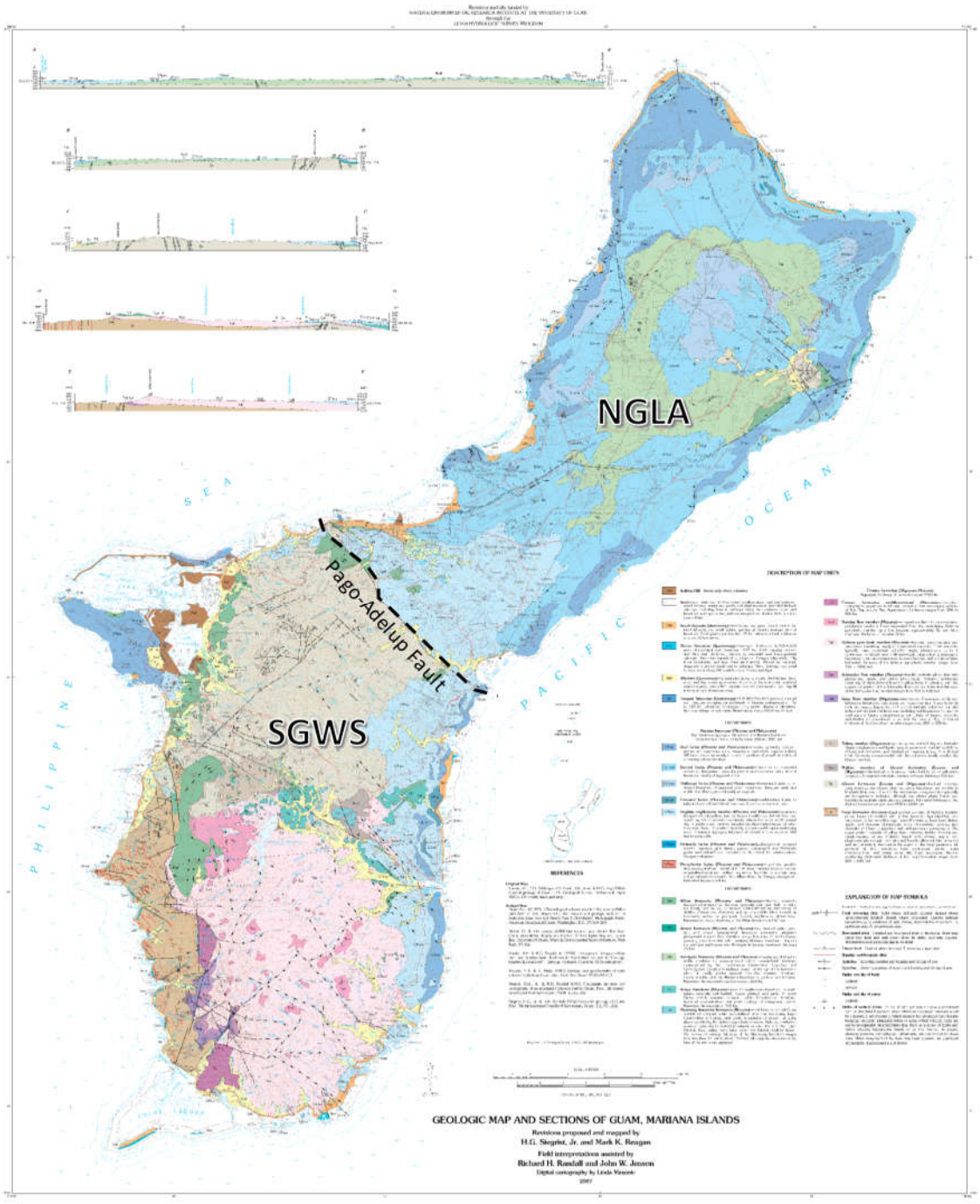

Appendix 1. Geologic Map and sections. The Pago-Adelup Fault divides the NGLA and Southern Guam, and the map shows the NGLA's limestone formation groups. https://guamhydrologicsurvey.uog.edu/wp-content/Maps/SiegristEtAl07-GeologicMapSectionsGuamMarianaIslands.pdf

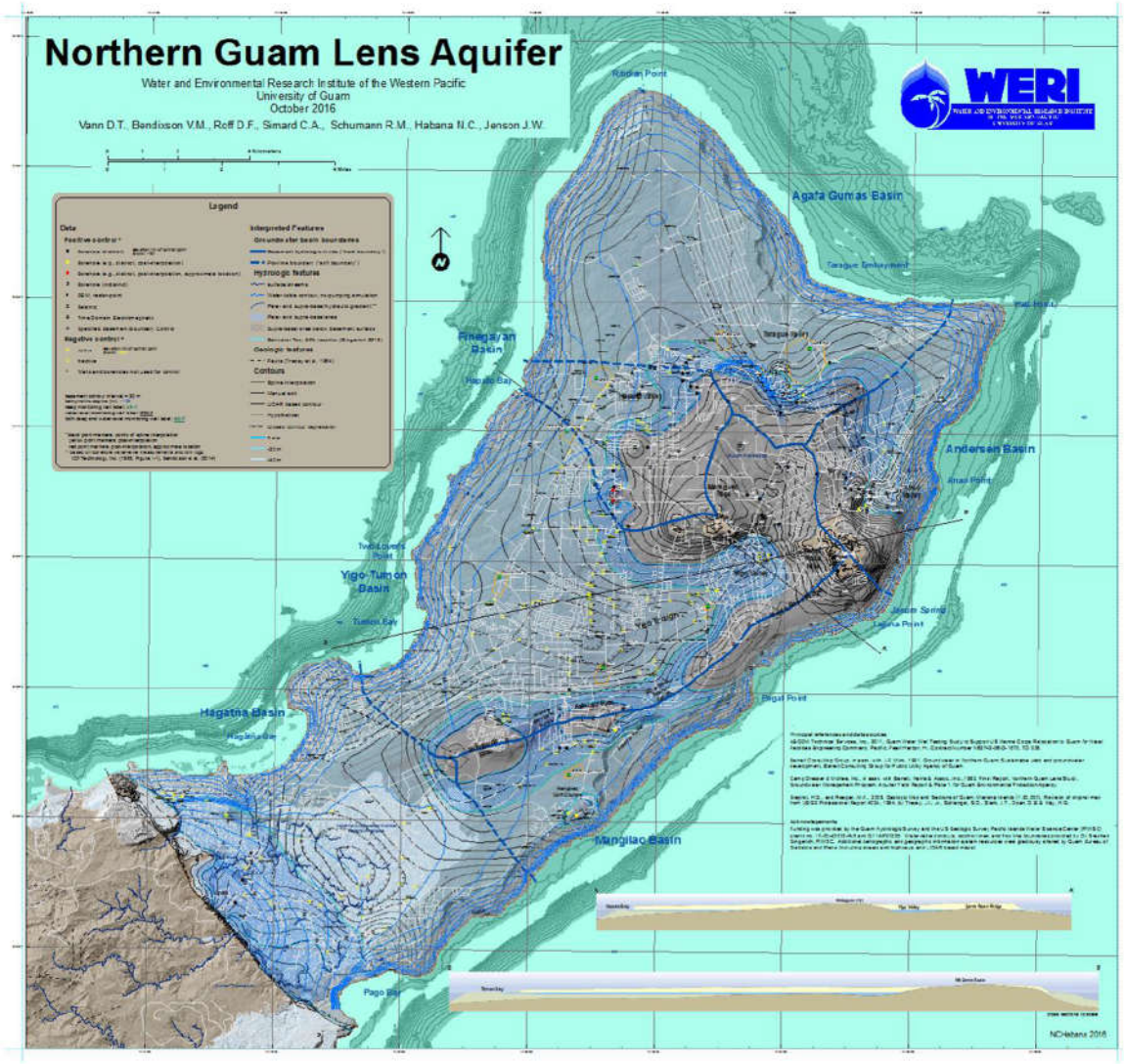

Appendix 2. The Northern Guam Lens Aquifer hydrogeologic map (Vann et al. 2014). Update 2019: https://guamhydrologicsurvey.uog.edu/wp-content/Maps/WERI2018-NGLAMap1.pdf